EurJOC
European Journal of Organic Chemistry

Review
doi.org/10.1002/ejoc.202301050

Chemistry Europe
European Chemical Societies Publishing

www.eurjoc.org

Synthesis of Cryptophanes: Recent Advances

Sindhu Kancherla[a] and Jørn H. Hansen*[a]

This review covers the latest developments in the synthesis of cryptophane host molecules since the publication of the last extensive review by Brotin and Dutasta in 2009. The literature has been categorized according to the synthetic method for generating the cryptophane core and we also emphasize emerging late-stage functionalization approaches. The synthetic strategies towards cryptophanes can be broadly categorized into the well-established direct- (two-step), template- and coupling (or capping) methods. The examples covered in this review mainly highlight template-based synthesis, coupling approaches and late-stage functionalization.

1. Introduction

Supramolecular chemistry has gathered considerable attention, particularly since the 1987 Nobel Prize award to Cram, Lehn and Pedersen in this area[1], and continues to be an active area of frontier research. Molecular host classes like cyclodextrins,[2] calixarenes,[3] cucurbiturils,[4] crown ethers,[5] metallacrowns,[6] cryptands,[7] pillararene,[8] cavitands[9] and cyclophanes[10] have been extensively studied. Cryptophanes are another example of a class of supramolecular host molecules, first synthesized by Collet in the 1980s.[11] These cage molecules consist of two cyclotribenzylene (CTB) units (Figure 1) joined together by three linker chains. Depending on the chirality (*P* or *M* configuration) of the CTB units present in the cryptophane, the structure can be assigned *anti* or *syn* configuration. The *syn*- and *anti*-diastereomers of cryptophanes tend to differ in their physicochemical and complexation properties. The chiroptical aspects of cryptophanes have been extensively reviewed by Baydoun and Brotin.[12]

CTB units can exist in crown or saddle conformations (Figure 1a).[13] Consequently, cryptophanes can have globular or imploded conformations (Figure 1b).[14] Factors such as length of linkers, the nature of solvent and guest molecules influence the conformational preferences in solution and the solid state.[15] The imploded conformations, particularly the out – saddle conformer, can be formed by the collapse of out – out conformers due to the evacuation of guest molecules at high temperature, particularly in solvents that are too big to occupy the cavity[15a] (although an exception of spontaneous isomerization has been reported[16]). The formation of imploded conformations can be reversed by reflux in a solvent suitable as a guest molecule.[17] The imploded cryptophanes are not efficient in encapsulating the guest molecules and they can complicate the synthesis process by making the purification and characterization of product mixtures difficult.

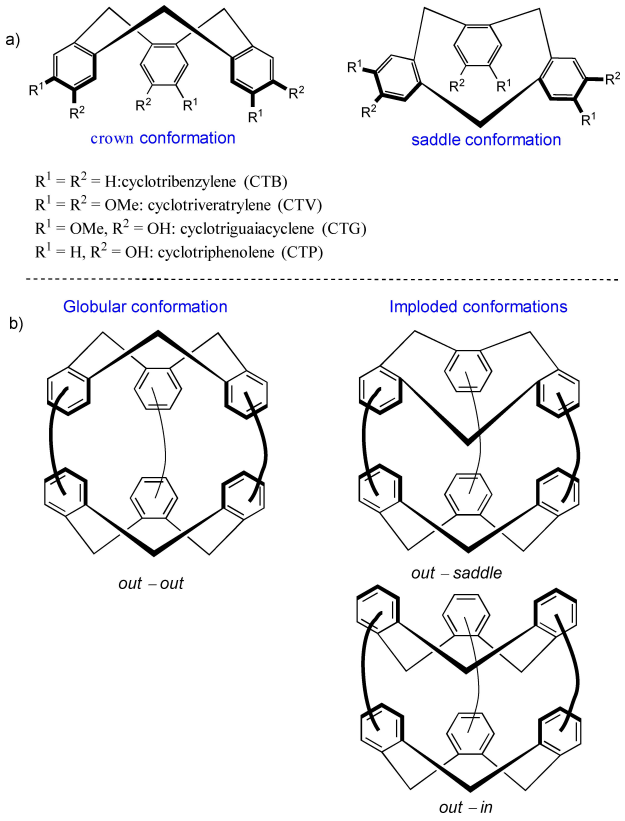

Figure 1. a) Commonly used nomenclature and conformers of CTB. b) Experimentally reported conformers of cryptophane.

The specific configuration of CTB units and the three linkers, form an internal lipophilic chiral cavity, whose volume is predominantly defined by the length of the linkers. This cavity makes cryptophanes a useful class of molecular hosts for applications in analytical and environmental chemistry and chemical biology.[18] Depending on the size of the cavity and size of apertures to access the cavity, cryptophanes can

[a] *S. Kancherla, J. H. Hansen*
Sindhu Kancherla and Jørn H. Hansen
Department of Chemistry,
Chemical Synthesis and Analysis Section
UiT The Arctic University of Norway
N-9037 Tromsø, Norway
E-mail: jorn.h.hansen@uit.no

accommodate guest molecules of suitable sizes, namely small-molecule gases CH_4,[19] Xe,[20] haloforms and chiral halomethanes such as CHFClBr, CHFClI,[21] chiral oxiranes,[22] cubane,[23] acetylcholine,[24] soft cationic species such Cs^+, Tl^+,[25] NH_4^+[24] and organic anions such as trifluoromethanesulfonate ($CF_3SO_3^-$).[26] Computational studies have been conducted to understand the NMR chemical shift changes of encapsulated CH_4 and Xe,[27] substituent modification in the host,[28] Xe-affinity,[29] complexation and exchange dynamics of Xe, and the role of solvent.[30] Due to the rigid structures of cryptophanes with or without guest molecules, and the availability of chiroptical information from experimental studies of their enantiopure forms, these cage molecules have been used as model molecules to demonstrate the applicability of quantum chemical calculations to confirm Vibrational Circular Dichroism (VCD),[31] and Raman Optical Activity (ROA) spectra.[32] The late-stage mono-functionalization of cryptophanes with biological ligands and fluorophores has enabled their potential applications as biosensors and in molecular imaging.[27–32,34]

The CTB intermediate has also been functionalized to obtain mono-, di- and tri-functionalized derivatives with their own potential applications.[35] Depending on the groups present on the aromatic rings of CTB, they follow a general nomenclature such as cyclotriveratrylene (CTV), cyclotriphenolene (CTP), cyclotriguaiacyclene (CTG) (Figure 1a), which is commonly used over complicated IUPAC nomenclature. Regarding cryptophanes, Collet named these compounds as cryptophane-A, B, C, D and so forth according to their chronological order of discovery.[13] As the structural diversity of cryptophanes kept on progressing, the old nomenclature became insufficient. Therefore, apart from the IUPAC nomenclature, they are commonly named by the number of methylenes (n) in the three alkyldioxy linkers. For example, cryptophane-111 indicates CTBs joined by three methylenedioxy linkers.

CTB molecules have been linked together with six linkers to form cryptophane-like molecular containers that can host dimethyldiazapyrenium, 4,4′-biphenylbisdiazonium ions and fullerenes.[36] The six linkers can be oligoethylene glycol chains or alkyldioxy chains as shown in Figure 2.

There are three major *de novo* synthetic strategies to obtain cryptophanes (Figure 3).[37] These macrocyclization approaches are typically not high yielding due to energetic and entropic constraints on both cyclization rate and structure of 22−28

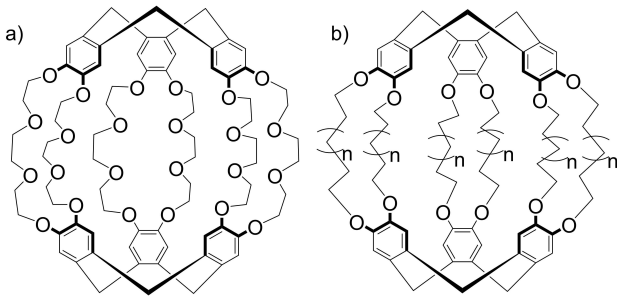

Figure 2. Cryptophane-like molecular containers with six linkers.

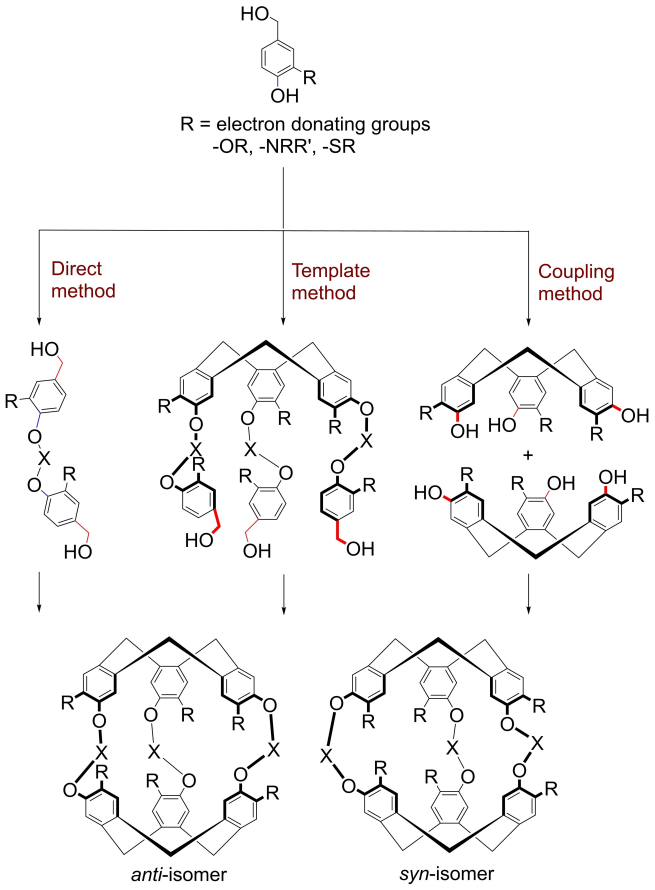

Figure 3. Synthetic strategies towards cryptophanes.

Prof. **Jørn H. Hansen** received his Ph.D. in organic chemistry from Emory University (USA) in 2010 followed by postdoctoral research at Princeton University, before joining UiT The Arctic University of Norway in 2012 where he is currently a full professor of chemistry. His research interests range from development and applications of novel late-stage functionalization methods, chemical library design with bioactive and functional heterocycles for medicine and materials, computational chemistry and chemical education.

Dr. **Sindhu Kancherla** obtained her MSc-degree in Chemistry from Nizam College (Osmania University, India) and received her PhD in Organic chemistry from the University of Stavanger, Norway (Assoc. Prof. Kåre Jørgensen group) in 2020 where she worked on synthesis and functionalization of polycyclic aromatic hydrocarbons. She then joined the group of Prof. J. Hansen at UiT, focusing research on the design, synthesis, and functionalization of novel CTBs and cryptophanes for potential applications in optical sensor technology.

membered rings. Among the three, the shortest approach is the *direct method* involving the formation of a bis-(benzyl alcohol) intermediate which can subsequently undergo axial trimerization, albeit typically in low yields. The direct method is further limited by the requirement of electron-donating groups (EDG) *meta* to the benzyl alcohol precursor in order to promote the trimerization or cyclization to form the two CTB units.[26b] Since the direct method is not much employed in later years, it is not covered herein. The *template method* is a multi-step strategy which offers flexibility to synthesize cryptophanes with various substituents. It is the only method that can facilitate the synthesis of cryptophanes with low symmetry without the need for late stage functionalization (LSF),[38] and has been employed widely in recent years to make a range of substituted cryptophanes as discussed in the next section. The third approach is the equatorial *coupling method*, although comparatively less time-consuming, it has clear limitations governed by steric clashes between rim-substituents (R groups) on the CTB units. The three strategies are still the predominant *de novo* strategies for constructing cryptophanes, however, LSF is emerging as an important strategy to obtain complex substituted cryptophanes for various applications. The synthesis of functionalized cryptophanes is an excellent arena for demonstrating the importance of late-stage functionalization chemistry since the parent frameworks can be challenging as well as time- and resource demanding to make. In this review, we have compiled most of the developments in both *de novo* and functionalization chemistry for the synthesis of cryptophanes since the last extensive review by Brotin and Dutasta in 2009.[39]

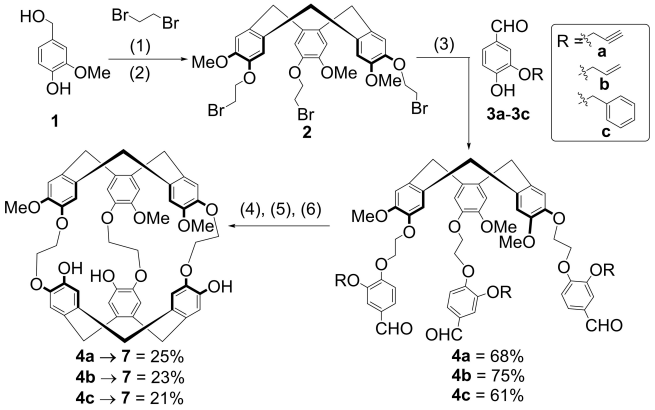

Conditions, reagents and yields:

1) K_2CO_3, DMF, 58%. 2) $Sc(OTf)_3$, CH_2Cl_2, 35 °C, 2 days, 67%.3) **3a-3c**, Cs_2CO_3, DMSO, 55 °C, overnight. 4) $NaBH_4$, (4:1) THF:MeOH, −10 °C to RT, 4 h (**5a** = 87%; **5b** = 82%; **5c** = 83%). 5) $Sc(OTf)_3$, CH_2Cl_2, reflux, overnight (**6a** = 42%; **6b** = 40%; **6c** = 35%). 6) Deprotection of —OR groups (**6a** → **7** = 68%, **6b** → **7** = 69%, **6c** → **7** = 72%).

Scheme 1. Synthesis of trifunctionalized cryptophane-A derivatives.

2. Synthesis of cryptophanes by the template method

The template method was previously considered a time-consuming multi-step synthesis of cryptophanes (Figure 2), involving the preparation of linker units and CTB templates. However, Brotin and co-workers made the synthesis of cryptophanes more economical with the use of $Sc(OTf)_3$ as a mild catalyst for the cyclization of benzyl alcohol derivatives.[40] For example, the previously reported synthetic methods have nine or more steps with low yields for the synthesis of trisubstituted cryptophane-A derivatives.[39] Dmochowski *et al.* reported a shorter synthesis in 2011 from commercially available vanillyl alcohol (**1**) with only six steps (Scheme 1).[41] The tri-(2-bromoethyl)-CTB **2** was prepared in two steps *via* S_N2 *O*-alkylation and $Sc(OTf)_3$ catalysed cyclization from **1**. The CTB **2** was further reacted with 4-hydroxybenzaldehydes (**3a**-**3c**) differentially substituted at the oxygen in the 3-position (propargyl, allyl or benzyl). The tri-aldehyde template precursors **4a**-**4c** were first reduced and then cyclized using $Sc(OTf)_3$ to afford trisubstituted cryptophane-A derivatives **6**. This approach was used to synthesize tripropargyl-cryptophane A (**6a**), triallyl-cryptophane A (**6b**) and tribenzyl-cryptophane A (**6c**) with five steps in the longest linear sequence. The cryptophane-A derivatives **6a**-**6c** were then transformed into trihydroxy cryptophane-A (**7**) thereby obtaining **7** in about 4% overall yield. Alternatively, the tri-aldehyde template precursor **4b** can be reduced and the allyl groups can be simultaneously deprotected using excess $NaBH_4$. After the final cyclization using $Sc(OTf)_3$ the **7** was obtained in only six steps from **4b** with an overall yield of 9.5%. Hyperpolarized ^{129}Xe-NMR chemical shifts were measured for these Xe@trifunctionalized cryptophane-A complexes in the range of 57–65 ppm.

The generation of enantiopure, trisubstituted cryptophane-A was reported by Dmochowski *et al.* in 2012.[42] The cryptophane **7** was resolved using (*S*)-Mosher's acid and the resulting diastereomers were separated using silica gel column chromatography, isolating each isomer in 35% yield. The ^{1}H-NMR spectra displayed chemical shift differences for aromatic protons in the two isolated diastereomers. Electronic circular dichroism (ECD) displayed similar peaks with opposite signs for the isolated diastereomers. Hyperpolarized ^{129}Xe-NMR chemical shifts of the corresponding Xe-complexes were measured to be 9.5 ppm apart. The removal of the Mosher auxiliaries provided the two enantiomers of cryptophane **7** in high enantiomeric excess. This approach enables access to new enantiopure trisubstituted cryptophane-A derivatives.

Rousseau *et al.* reported the synthesis of highly water-soluble, substituted cryptophanes bearing poly(ethylene glycol) (PEG) chain substituents (Scheme 2).[43] The template approach starts by protecting the phenol group in commercially available **1** with PEG-550 **8**, followed by trimerization to form CTB **9** in 50% yield. The methoxy groups in CTB **9** were deprotected using $LiPPh_2$,[44] which was then split and treated with **10a** and **10b** to form the CTB templates **11a**-**11b**, both in 20% yield. The cyclization of templates **11a**-**11b**, in the presence of formic acid resulted in the formation of PEGylated cryptophanes **12a**-**12b**. The overall yield of cryptophane **12a** formed over five steps was 3%. As an example of LSF, cryptophane **12a** underwent a copper(I)-catalyzed [3 + 2]-cycloaddition with azide

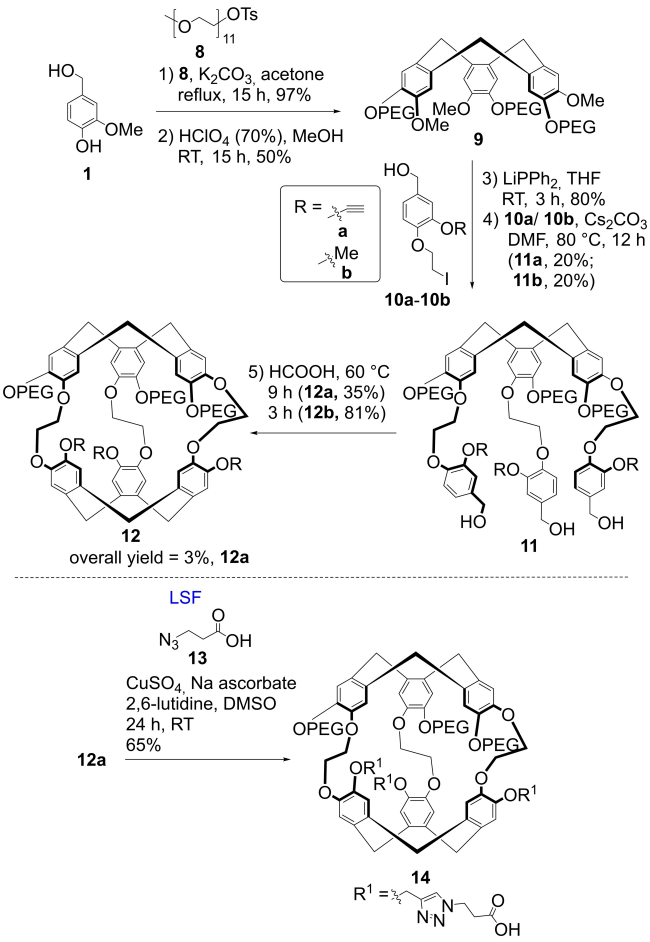

Scheme 2. Synthesis of PEGylated cryptophane-222 and LSF *via* click-chemistry.

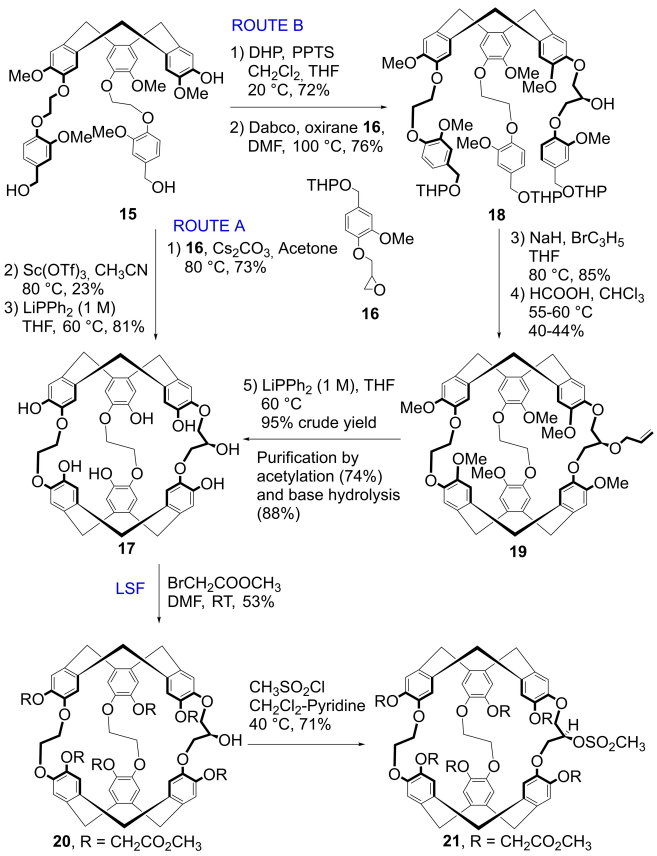

Scheme 3. Synthesis of a cryptophane-223 scaffold with a secondary alcohol on one linker and an example of LSF *via* S_N2.

13 to afford tri-functionalized cryptophane **14** in 65% yield. The PEGylated cryptophanes exhibited high affinity for Xe and are suitable for ^{129}Xe-NMR biosensing studies.

Brotin and co-workers reported a strategy to synthesize more hydrophilic cryptophane-223 structures with lower C_1 symmetry (Scheme 3),[45] in which the equatorial linkers consist of two ethylenedioxy- and one propylenedioxy-linkers. If the two CTB caps possess the same absolute configuration (*M* or *P*), the central carbon of the propylenedioxy-linker will not be a stereogenic center. The central hydroxy group in the propylenedioxy linker can be employed to introduce substituents on the cryptophane without leading to structural complexities and in turn allows the introduction of additional fragments or ligands different from those present on aromatic rings. The synthetic approach is similar to a previously published procedure by Dutasta *et al.* to afford C_2-symmetric cryptophanes-223, −233 and −224, *via* step-wise functionalization of CTB with different linkers.[38] Following route A, bis-functionalized CTB **15** with two ethylenedioxy linkers[46] was subjected to S_N2 alkylation with epoxide **16** to obtain the corresponding CTB-template (73%). This step resulted in the generation of the secondary alcohol on the propylenedioxy linker. For the cyclization of the CTB template, formic acid conditions failed to promote the formation of product presumably due to the reaction of the unprotected secondary alcohol with formic acid. When $Sc(OTf)_3$ was employed the *anti*-product was formed in 23% yield in route A. To improve the yield, a second strategy was attempted (Scheme 3, route B) consisting of two additional steps of protecting two benzylic alcohols in CTB **15** with 3,4-dihydro-2H-pyran (DHP) and the secondary alcohol in CTB template **18** with allyl bromide. The presence of THP groups in CTB **18** results in a complex mixture of diastereomers. After the cyclization under formic acid conditions, the complex mixture of diastereomers of CTB **18** is transformed into the two enantiomers of cryptophane **19** as a racemic mixture in 40–44% yield. After deprotection of the methoxy groups, the cryptophane **17** provides six phenolic groups apart from the secondary alcohol group for the synthesis of various derivatives. The C_1-symmetric cryptophane **17** was obtained from CTB **15** in an overall yield of 14% following route A and 12% following route B. Illustrating LSF, the six phenolic groups of the cryptophane-223 core were transformed into esters (**20**), carboxylic acids, and PEG groups. The secondary alcohol on the linker of the hexa-ester cryptophane-223 (**20**) was transformed to a methyl sulfonyl group to obtain cryptophane **21** in the presence of pyridine (71% yield). ^{129}Xe-NMR studies of **17** and its LSF-derivatives showed slow exchange on the NMR time scale. In another study by Brotin, Buffeteau and co-workers, the LSF derivative of **17** bearing seven acetate groups displayed self-encapsulation of

the acetate group on the propylenedioxy linker in 1,1,2,2-tetrachloroethane and dimethylsulfoxide (DMSO) solvents.[47] However, in the presence of competing solvent such as CH_2Cl_2, the acetate moiety remained outside the cavity. Another derivative of **17** bearing six methoxy groups on the aromatic rings and acetate group on the propylenedioxy linker, also showed similar self-encapsulation of acetate moiety but has different chiroptical properties.

Brotin and co-workers utilized the above discussed strategy to generate a more accessible primary alcohol on the cryptophane-223 core. Two consecutive S_N2 reactions of CTG **22** with vanillyl alcohol derivatives **23** and **24** generated the required CTB template **25** (Scheme 4).[48] After cyclisation of the CTB template **25** to the cryptophane-223 core **26** in 40% yield, the alkene was transformed into a primary alcohol in **27** through a hydroboration-oxidation reaction using 9-borabicyclo(3.3.1)nonane (9-BBN). X-ray crystallography of **27** confirmed the *anti*-configuration. The cryptophane **28** contains six methoxy groups and one −THP protected primary hydroxy group available for selective deprotection and transformation to water soluble functional groups. For instance, in **28** the six methoxy groups can be selectively transformed into ester derivatives (**29**, and **30**). The primary alcohol in **29** and **30** was successfully oxidized *via* the Dess-Martin reagent to obtain cryptophanes **31** and **32** respectively. The free carboxylic acid group in **31** was subjected to $POCl_3$-mediated amide coupling with *O*-benzylhydroxylamine (**33**) and subsequent hydrogenolysis to prepare cryptophane-223 with a hydroxamic acid functional group (**34**) enabling metal chelation towards Ni^{2+} and Zn^{2+}. Isothermal titration calorimetry demonstrated efficient binding of the host **34** and metal ions at neutral pH.

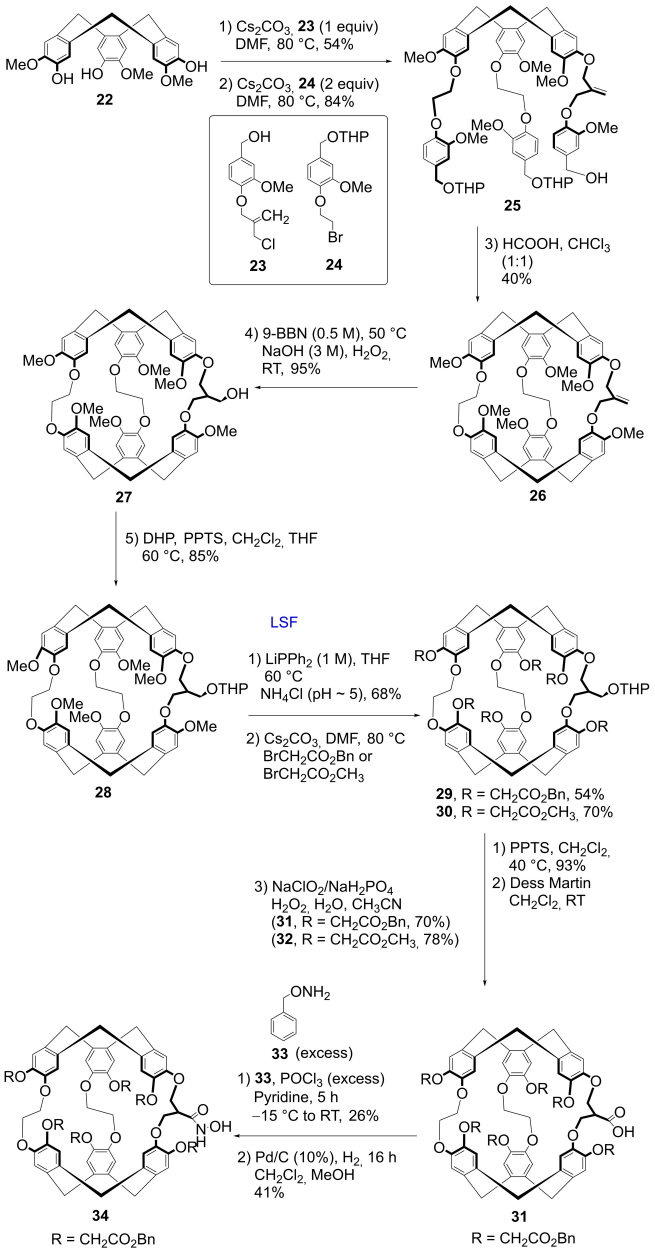

Scheme 4. Synthesis of cryptophane-223 with a primary alcohol on the linker and subsequent LSF.

Brotin and Buffeteau *et al.* reported the synthesis of a highly substituted cryptophane core with nine and twelve methoxy substituents from syringyl alcohol **35**, as shown in Scheme 5.[49] In the presence of $Sc(OTf)_3$, allylated syringyl alcohol derivative was cyclized to cyclotrisyringyl derivative **36** (CTS) in 20% yield along with cyclotetrasyringyl derivative **37** (CTTS, 7% yield). The other conditions such as $HClO_4$ and $SnCl_4$ failed to give any CTS product. The X-ray structure of **36** showed a triclinic P1 space group structure with four molecules per unit cell. The deprotection of allyloxy groups generated the tri-phenol CTS **38**, which was used to prepare the template intermediate and subsequently, cryptophane-222 with 12-methoxy groups *anti*-**41** and *syn*-**42** in moderate yields as shown in Scheme 5. The *anti*-cryptophane **41** is a chiral compound with D_3 symmetry, while the *syn*-cryptophane **42** is achiral with C_{3h} symmetry. Cryptophane-222 with nine methoxy substituents was also synthesized using two separate methods, A and B, from CTS **38** and from CTG **22** respectively. The *anti*-isomer **43** was obtained in similar yields from these two methods, whereas the *syn*-isomer **44** was obtained in slightly higher yield using method B. The presence of two methoxy groups on either side of the linker contributed to a significant increase in the formation of *syn*-isomer. Both these diastereomers are chiral and C_3-symmetric compounds. Small spectral differences in the region 1700–900 cm^{-1} were noticed in the experimental IR spectra of *anti*-**43** and *syn*-**44**. Considering the ambiguity of experimental IR data, X-ray crystallography was used to determine the stereochemistry of all the four cryptophane molecules **41**–**44**. Nevertheless, the anti- and syn- isomers (**41** and **42**, **43** and **44**) were purified by HPLC and the chiroptical properties of enantiopure cryptophanes were characterized.[50]

Brotin *et al.* reported the first synthesis of the *syn* diastereomer of cryptophane-A, traditionally named cryptophane-B, following a thirteen step route in 2018 (Scheme 6).[51] In this molecule, the two CTB units of opposite absolute configurations (*M*, *P*) are connected by three ethylenedioxy linkers and the resulting cryptophane B is therefore of C_{3h} symmetry. The known tribenzyloxy-CTB **45** and (3-(allyloxy)-4-(2-bromoethoxy)benzyl alcohol **46** were used to synthesize a CTB template bearing 3-allyloxybenzyl alcohol groups. This CTB template

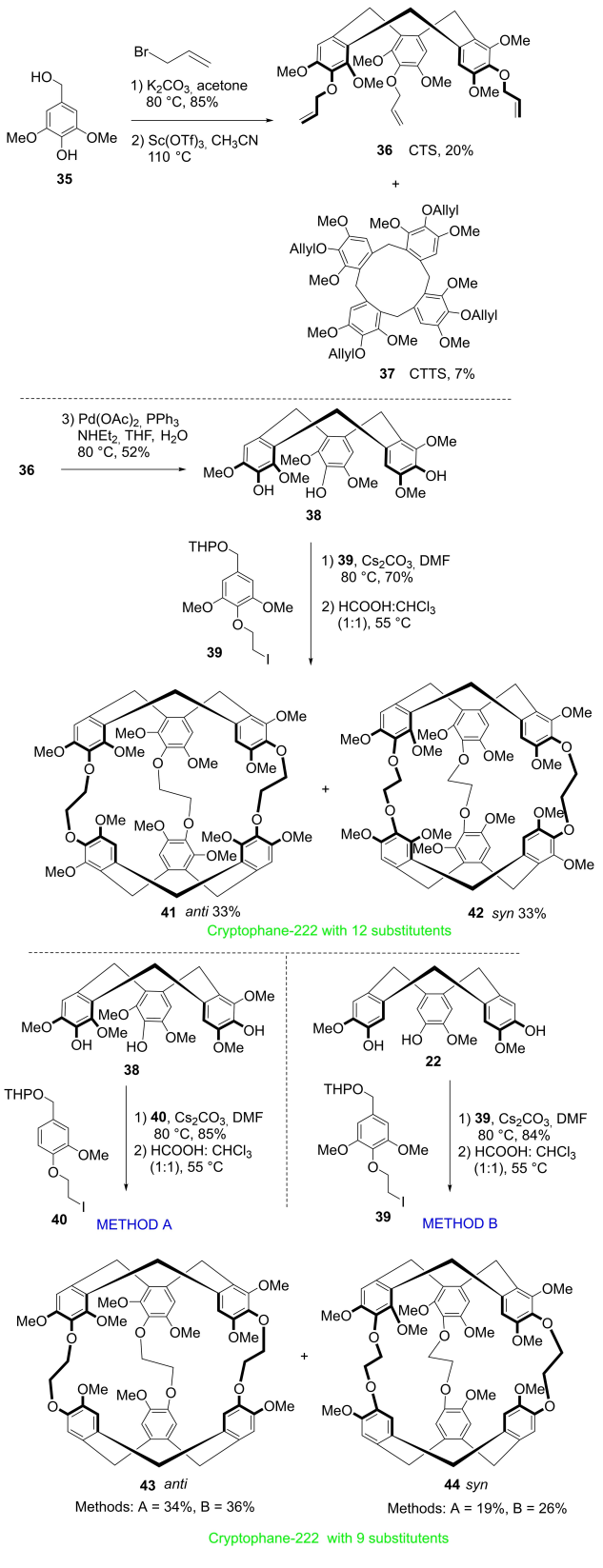

Scheme 5. Synthesis of cryptophane-222 with twelve and nine methoxy substituents.

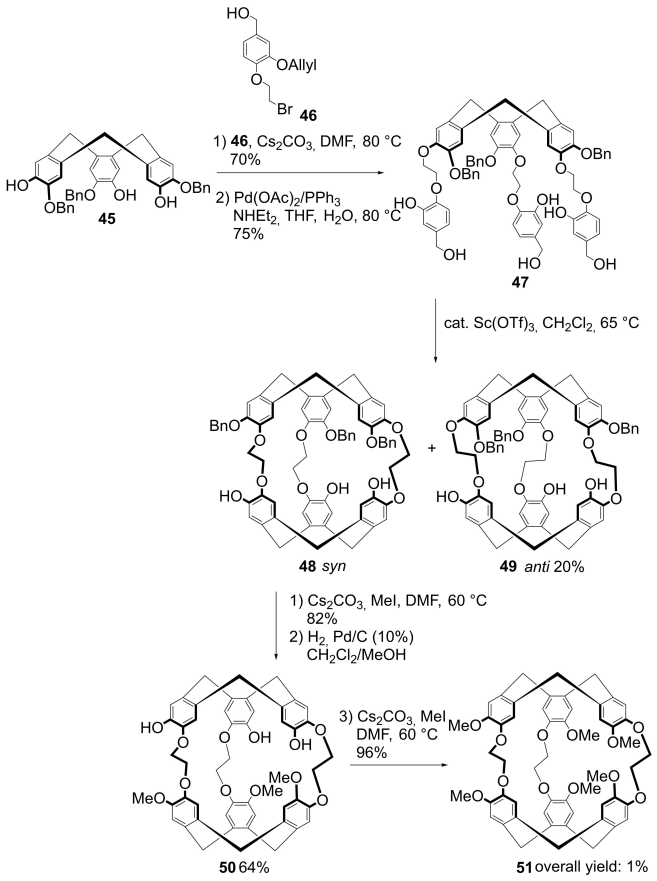

Scheme 6. Synthesis of cryptophane-B.

failed to cyclize both under acidic conditions and using $Sc(OTf)_3$. The reactions resulted in the formation of polymeric materials due to the presence of allyloxy groups. Therefore, the allyloxy groups were deprotected to afford template **47**, which was then successfully cyclized using catalytic $Sc(OTf)_3$ resulting in the formation of cryptophanes *syn*-**48** and *anti*-**49**. ^{1}H-NMR of crude product mixture showed the *anti*- and *syn*- isomers were obtained in a 75:25 ratio. The cryptophane **48**, which is an important intermediate with the *syn* relative configuration, has been isolated in low yield. Further transformation of **48** afforded cryptophane-B (**51**) in three steps. Brotin and Berthault *et al.* prepared a water soluble cryptophane with three OH groups and three carboxylic acid groups (**52**) from *anti*-**49**, to study the potential application of **52** as a pH sensor (Scheme 7a, route A).[52] The group also studied the selective capture of Tl^+ and Cs^+ ions by **52** in aqueous solution (Scheme 7a, route A and B).[53] In the latter study, the synthetic pathway of route B generated the imploded form of the cryptophane in significant amount, which does not have any efficient binding properties. In another study by Brotin *et al.* the *syn*-isomer **48** underwent hydrogenolysis in 83% yield and **53** was used to study the binding properties with Cs^+ and Tl^+ ions (Scheme 7b).[54] Berthault *et al.* transformed the *syn*-isomer **48** in to a water-soluble hexacarboxylic acid substituted cryptophane **54** in a stepwise manner, using methyl bromoacetate.[55] The *syn*-**54** displays a high binding constant towards Xe. Brotin and

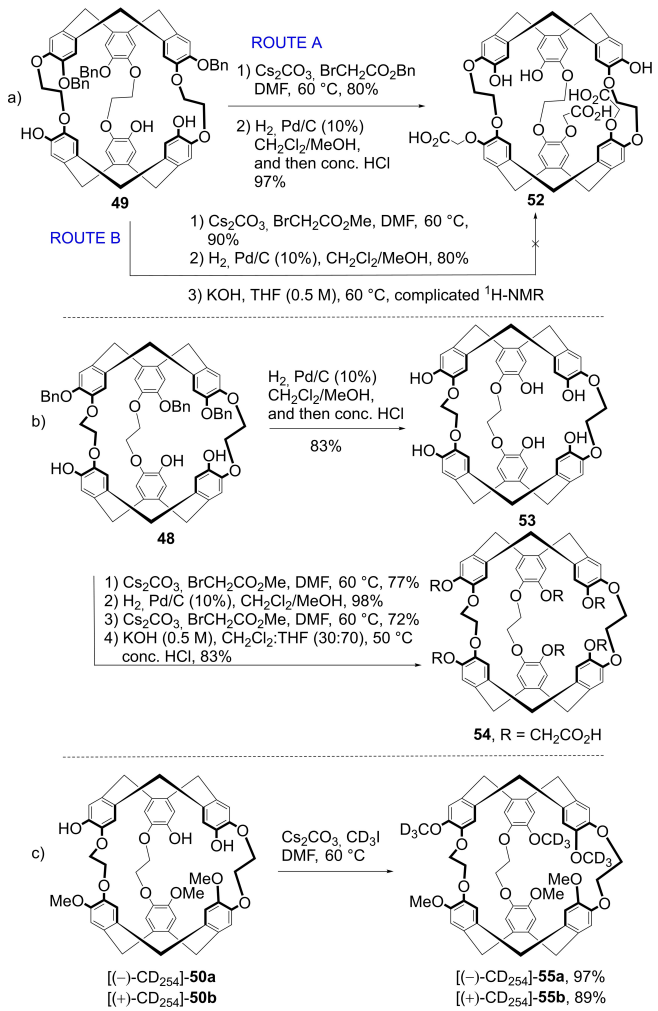

Scheme 7. Functional group interconversions of triphenolic cryptophane-222.

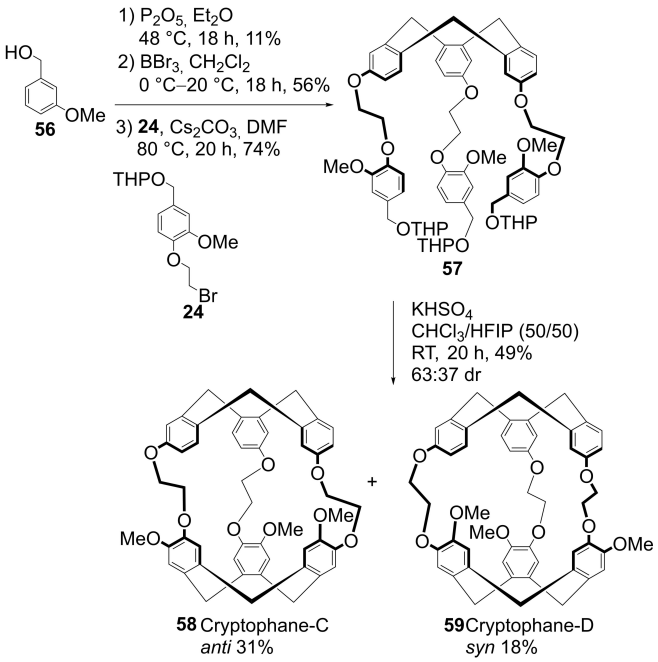

Scheme 8. Synthesis of cryptophanes C and D using HFIP as co-solvent.

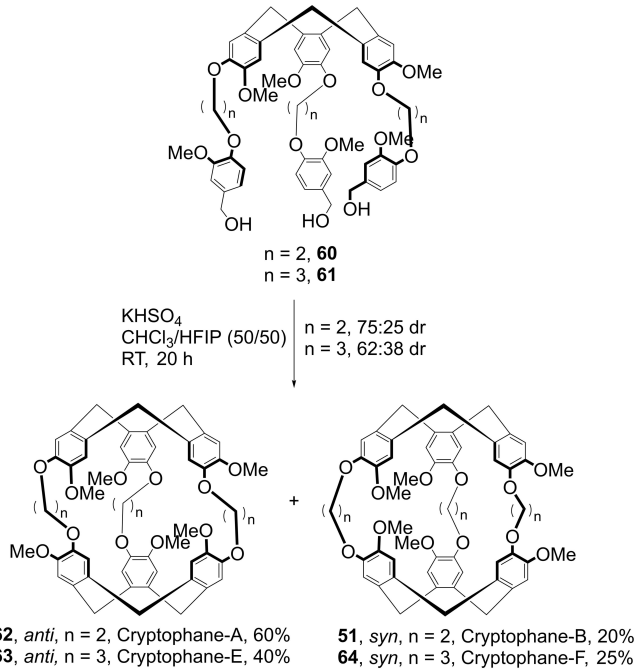

Scheme 9. Synthesis of cryptophanes A–B and E–F using HFIP/$KHSO_4$.

Buffeteau *et al.* reported the synthesis of enantiopure chiral isotopologues **55a** and **55b** from enantiopure achiral **50a** and **50b** *via* S_N2-reaction using CD_3I (Scheme 7c).[56] Before the reaction, the enantiomers **50a** and **50b** were separated on semipreparative chiral HPLC column, although optical resolution was the preferred method. The absolute configuration of the two enantiomers **50a** and **50b** was determined by chiroptical techniques such as polarimetry, ECD, VCD and ROA.

A study conducted by Martinez and co-workers in 2022 disclosed the use of 1,1,1,3,3,3-hexafluoroisopropanol (HFIP) as a co-solvent in the presence of $KHSO_4$, for the final cyclization of the template intermediate. The HFIP co-solvent seemed to affect the regioselectivity and yielded both *anti*- and *syn*-diastereomers of various cryptophanes such as A–B (**62**, **51**, n = 2), C–D (**58**, **59**, n = 2) and E–F (**63**, **64**, n = 3) in different diastereomeric ratios (Schemes 8 and 9).[57] Previous studies using either formic acid[58] or $Sc(OTf)_3$[40] for the final ring closure step of the CTB template afforded mixtures of diastereomers **58** and **59** in ratios 83:17 and 86:14, respectively, with **58** as the major product. The *syn* cryptophane **59** was isolated in 5% yield under formic acid and 8% yield using $Sc(OTf)_3$ conditions. Compared to these previous methods, the HFIP/$KHSO_4$ combination resulted in the formation of **59** in 18% yield (Scheme 8). The reaction was found to be irreversible and under kinetic control from additional experimentation. By employing these new conditions in the template method, cryptophanes **64** and **51** were formed together for the first time in the same reaction in a diastereomeric ratio of 75:25 (Scheme 9). Notably, cryptophane **51** was isolated in 20% yield from this reaction

and an overall yield of 3% over five steps starting from vanillyl alcohol, demonstrating an improvement compared to the synthesis described in Scheme 6. Using formic acid conditions, the *syn* diastereomer **64** was reported in 50% yield,[26b] while the HFIP/$KHSO_4$ conditions afforded the diastereomer in 25% yield. Titration experiments supported the hypothesis that there might be interactions between **60** and HFIP influencing the regioselectivity of the cyclization reaction. However, the high cost of HFIP might be a disadvantage in the widespread usage of this approach.

Purohit *et al.* reported the synthesis of triazole-bridged cryptophanes by using the CuI-catalyzed click reaction (Scheme 10).[59] The synthesis was first attempted *via* the coupling approach, for which two CTB units tripropargyl-CTB **65** and triazide-CTB **67** were prepared from **1**. The CTBs **65** and **67** were subjected to click reaction conditions aimed at generating the triazole-bridged cryptophane. However, the reaction resulted in an insoluble white solid with only traces of the desired product. Subsequently, the template approach was employed in which 3-azidopropoxy-4-methoxybenzyl alcohol (**68**) was prepared in two steps from **1**. A click reaction between **68** and **65** afforded the triazole-bridged CTB template **69**. The cyclization of benzylic hydroxy groups in the triazole-bridged CTB template **69** turned out unsuccessful using various conditions such as $HClO_4$, $Sc(OTf)_3$ and BF_3-Et_2O in CH_2Cl_2. Changing the reaction conditions to BF_3-Et_2O in CH_3CN resulted in the formation of *anti*-**70** and *syn*-**71** isomers of triazole-bridged cryptophane. X-ray crystallography studies were conducted on *syn*-isomer **71** with tetraethylammonium cation as the guest molecule.

Brotin and De Rycke reported the first template-based synthesis of *syn*- and *anti*- tris-aza-cryptophanes in 2021.[60] The triamido-CTB **74** was prepared following two routes, A (step 1−3, known)[61] and B (Scheme 11), from 4-amino-3-methoxybenzyl alcohol **72** in 34% and 60% overall yields, respectively. The triamido-CTB **74** was treated with protected vanillyl alcohol **76**, and subsequent reduction of the amide afforded tris-aza-CTB template **78** in moderate 38% yield (Scheme 12). The final cyclisation step was conducted in a mixture of $HClO_4$/AcOH. The crude mixture was purified on silica gel and recrystallized to afford *anti*-tris-aza-cryptophane **79** in 1.2% yield and *syn* isomer **80** in 6% yield. Additional experiments to improve the yield of the cyclization step by using $HClO_4$ in MeOH afforded only small amounts of products. Other conditions such as formic acid in $CHCl_3$ or $Sc(OTf)_3$ did not result in cryptophane formation. The relative and absolute configurations were assigned using VCD and density functional theory (DFT) calculations. In the ^{129}Xe-NMR spectra at 11.7 T and 293 K, compared to their structural analogues cryptophane A (*anti*-**62**) and cryptophane B (*syn* **51**), **79** and **80** displayed two sharp signals indicating a slow in-out exchange dynamics of Xe. This strong effect on the in-out Xe exchange rate was hypothesized to be linked to the propensity of aromatic amine groups to

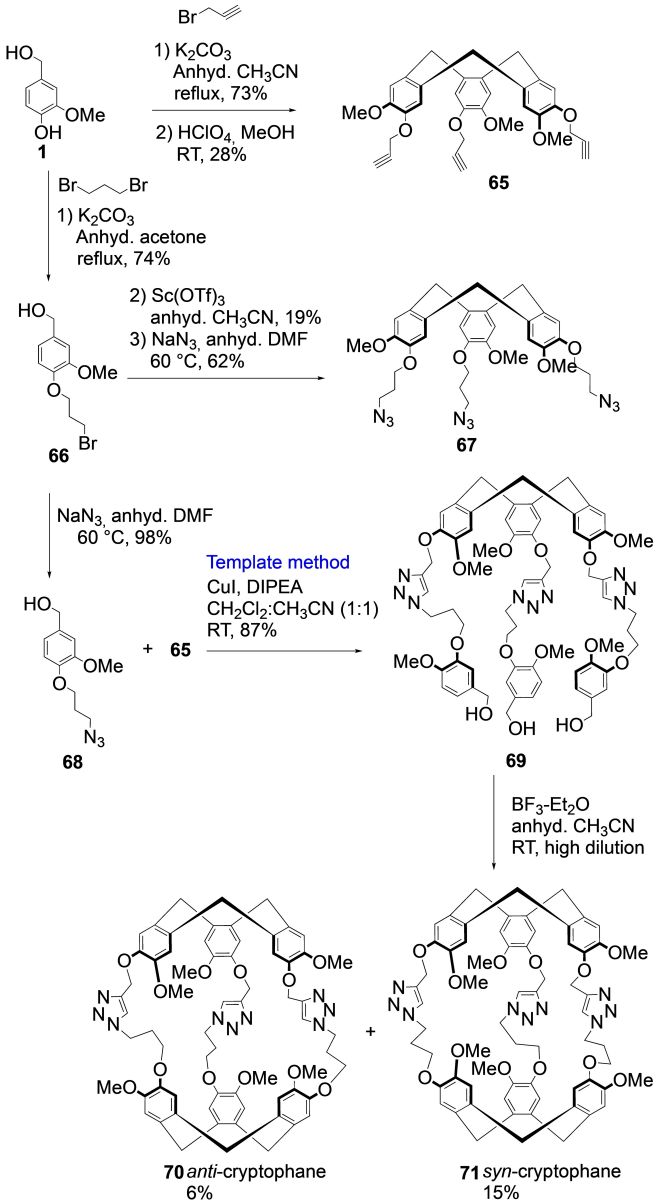

Scheme 10. Synthesis of triazole-bridged cryptophanes.

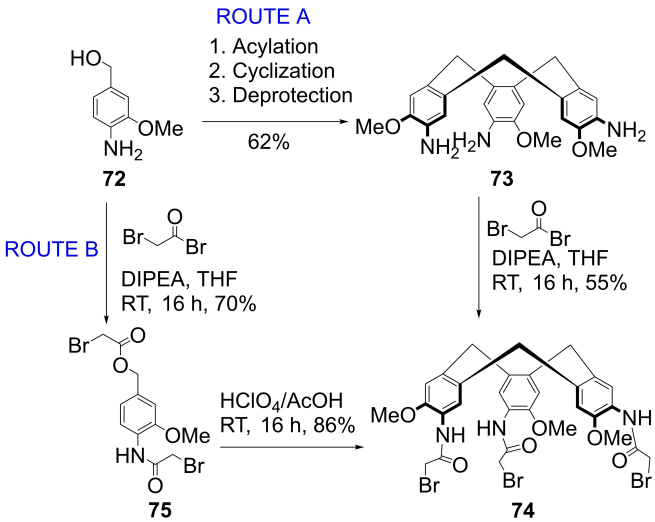

Scheme 11. Synthesis of triamido-CTB precursor.

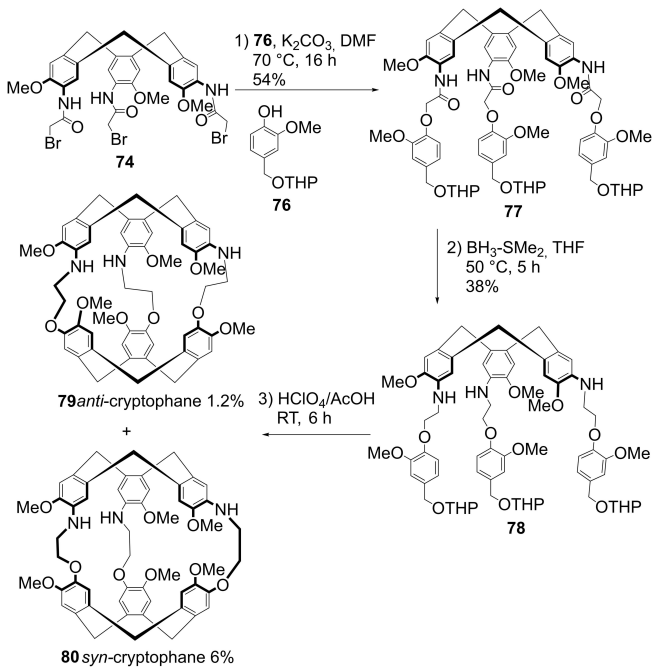

Scheme 12. Synthesis of trisaza-cryptophanes.

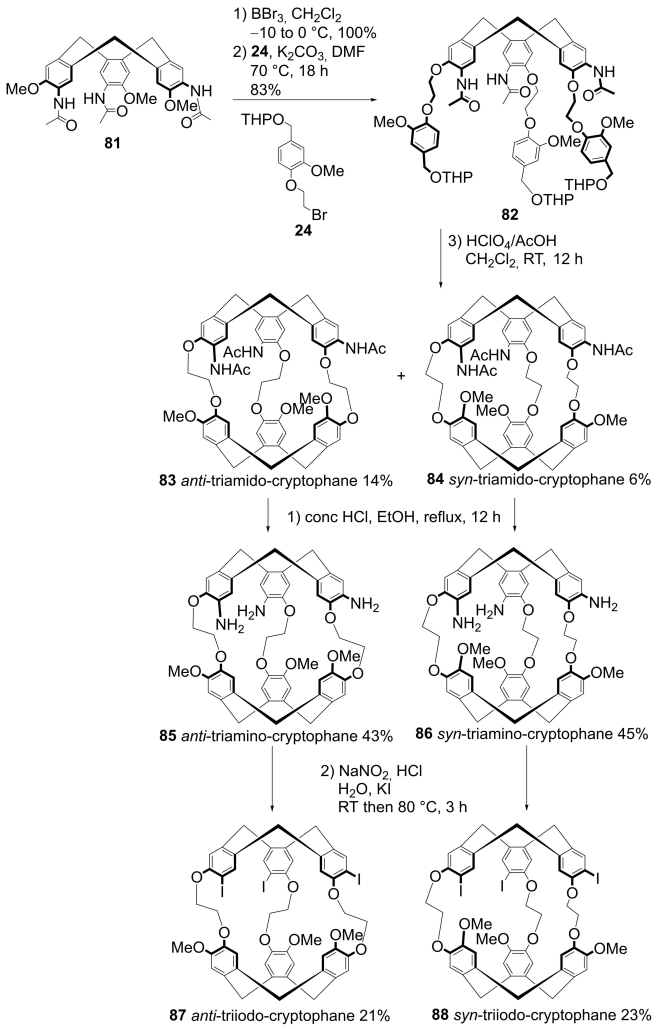

Scheme 13. Synthesis of triamido-, triamino- and triiodo- substituted C_3-symmetric cryptophanes.

form hydrogen bonding with residual water molecules. Interestingly, upon acidification with trifluoroacetic acid (TFA), the electron-donating properties of aromatic amines can be switched to electron-withdrawing, and the protonation might annihilate the water clusters near the portals of **79** and **80**. As a result, an increase in the in-out Xe exchange rate was observed when the medium was acidified.

The same group further developed the synthesis of *N*-containing cryptophanes in 2022, by reporting the synthesis of C_3-symmetric *syn*- and *anti*- cryptophanes with three aromatic amines on one of the CTB units (Scheme 13).[17] These molecules were prepared from the known triamido-CTB **81**, which was subjected to demethylation followed by the reaction with an excess of **24** to obtain CTB template **82** in 83% yield. The final ring closing reaction in CTB template **82** was conducted in the presence of a mixture of $HClO_4$/AcOH at room temperature to obtain *anti*- and *syn*-diastereomeric cryptophanes **83**, and **84** in 14% and 6% yields respectively. The acetanilide functional groups on **83** and **84** were deprotected separately by refluxing in HCl/EtOH, which afforded *anti*-**85** and *syn*-**86** diastereomers of triamino-cryptophane in 43% and 45% yields, respectively. ^{1}H-NMR spectra of heterocapped **85** and **86** have four singlet signals in the 6.9−6.4 ppm region showing four different aromatic protons and four doublets corresponding to the H_{ax} and H_{eq} of the methylene bridges owing to the presence of two differently substituted CTB units. The amino-groups can be substituted with iodo groups *via* a Sandmeyer-type reaction using $NaNO_2$/HCl and KI to obtain *anti*-**87** and *syn*-**88** triiodo-cryptophanes. The cryptophane **87** was isolated in a reversible imploded conformation and dissolution in $CHCl_3$ at reflux restored the globular conformation. Similar to trisaza-cryptophanes **79** and **80**, the ^{129}Xe-NMR studies of **83**–**86** at 11.7 T and 293 K indicated a slow Xe exchange regime with two separate signals observed each corresponding to free Xe and encapsulated Xe in the solution. The slow Xe exchange dynamics of **83**–**86** were attributed to the formation of water clusters near the portals because of hydrogen bonding with the nitrogen atoms (residual water in the solvents). The hypothesis was supported by 2D-EXSY experiments. Like for the majority of cryptophane-222 congeners, the^{129}Xe-NMR spectrum of the *anti*-**87** showed two signals, one each for free Xe in the solution at 223 ppm and Xe@**87** signal at 72 ppm, while the *syn*-**88** showed only one broad signal at 221.9 ppm corresponding to free Xe in the solution indicating a fast exchange regime.

Dubost and Cailly demonstrated the synthesis of cryptophazane, a cryptophane in which one of the axial methylene bridges has been replaced with an −NH group (Scheme 14).[62] The 2-amino-benzyl alcohol derivative **89** was first protected with TBDMS group before subjecting it to Buchwald-Hartwig amination (BHA) with **90** which afforded **91**. Deprotection followed by cyclization in $HClO_4$ resulted in the formation of intermediate **92**, a C_1-symmetrical CTB-1 N in 60% overall yield

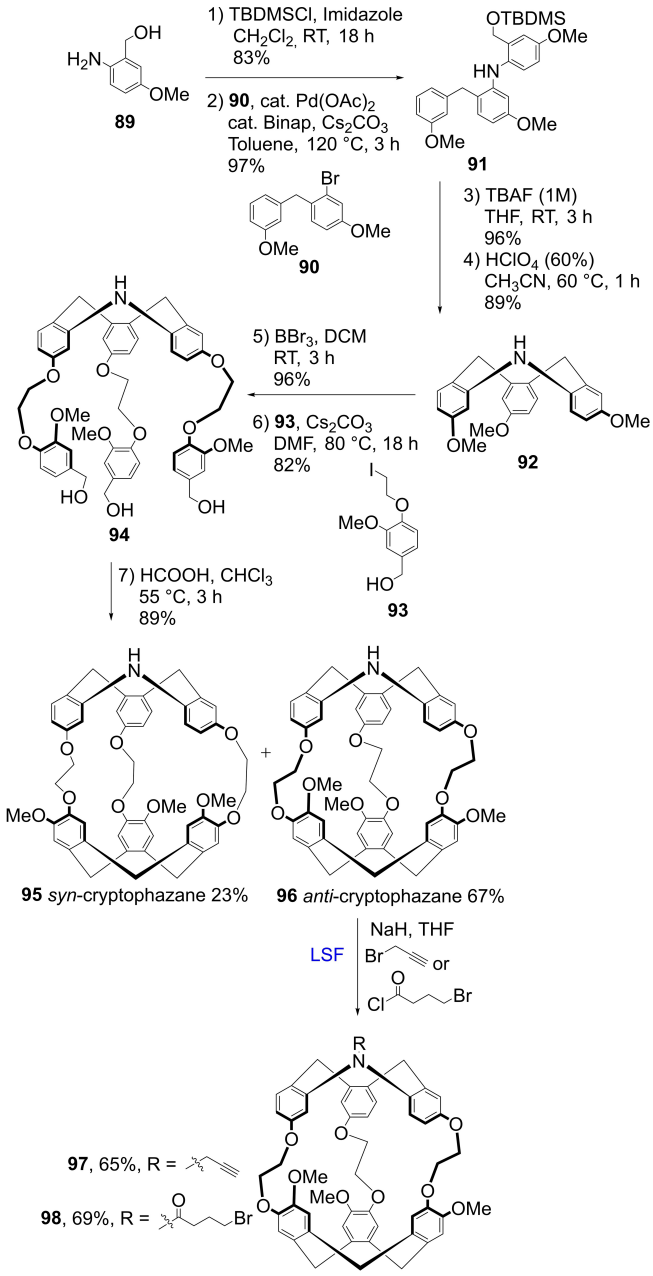

Scheme 14. Synthesis of cryptophazane.

in six linear steps from 2-amino-5-methoxybenzoic acid. The bromo-compound **90** for BHA was prepared by Barluenga Boronic Coupling (BBA).[63] X-ray crystallography confirmed the saddle conformation of CTB-1 N **92**. The methoxy groups in **92** were deprotected and subjected to *O*-alkylation with **93** to obtain CTB-1 N template **94**. The final cyclization step of **94** was conducted in formic acid in chloroform to obtain a mixture of *syn*-**95** and *anti*-**96** cryptophazane in 89% yield in the ratio 23:67 respectively. The conformations were assigned by X-ray crystallography. The −NH site in *syn*-**95** and *anti*-**96** can be used for LSF as illustrated for *anti*-**96**. The ^{129}Xe-NMR studies *anti*-**96** gave a residence time of 1.3 ms at 278 K for Xe inside the cavity. The solubility of *anti*-**96** increased exceedingly in CH_3CN, $CHCl_3$ and DMSO.

3. Synthesis of cryptophanes by the coupling approach and subsequent functionalization

3.1. S_N2- mediated coupling of CTB

A relatively short scalable synthesis of Cryptophane-111 was first reported by Rousseau *et al.* in 2010 (Scheme 15).[64] The synthesis comprises of five steps and generated the product in 12% overall yield. Cryptophane-111 (**102**) was obtained in 46% yield by heating CTP **101** with excess of Cs_2CO_3 and $ClCH_2Br$. The CTP **101** was synthesized from the commercially available 4-iodo-3-hydroxybenzyl alcohol **99** in four steps involving protection, trimerization, hydrodeiodination and hydrogenolysis. However, a much shorter scalable synthesis of CTP **101** from *meta*-methoxy benzyl alcohol **56** was reported by the same group in 2011.[65] The group also reported some examples of LSF of **102**, such as mono-iodination and mono-bromination.

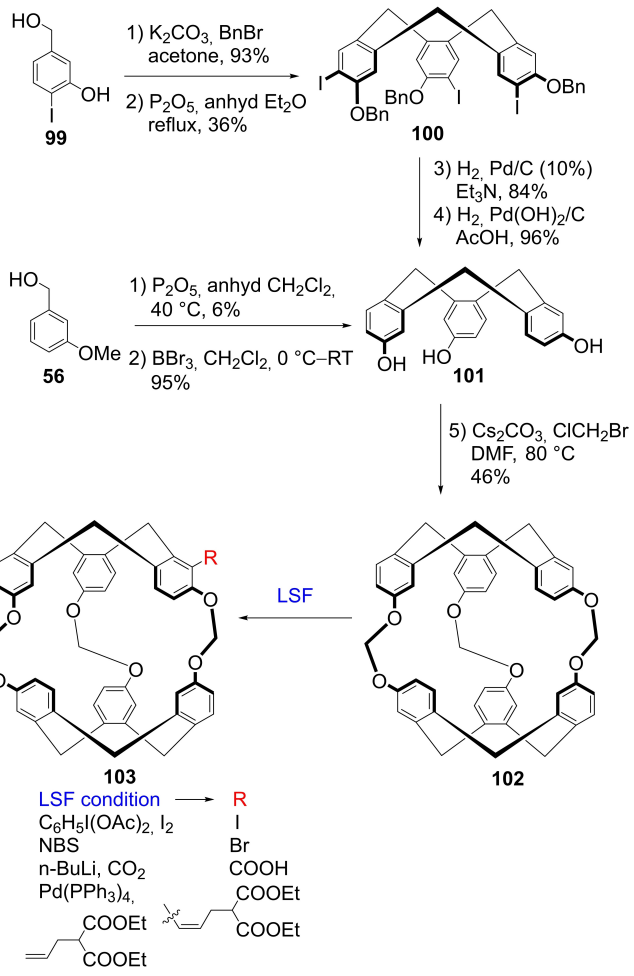

Scheme 15. Synthesis of cryptophane-111 and its LSF.

These mono-halogenated compounds were subjected to carboxylation *via* organolithium reaction and a Heck-coupling.[64]

The first examples of rim-functionalized cryptophane-111 were reported by Holman *et al.* in 2014 by employing the heterocapping or coupling method (Scheme 16).[66] In two separate experiments, the CTP **101** was reacted with excess of tribromo-CTB **104** and excess of CTG **22** in the presence of bromochloromethane to afford the formation of cryptophanes. The Br_3-cryptophane-111 (**105**) and $(MeO)_3$-cryptophane-111 (**106**) were obtained in 17% and 18% yields, respectively. X-ray crystallography confirmed the formation of *anti*-diastereomer in both cases. The homodimeric hexa-substituted side products were also observed in minor amounts, likely due to the steric crowding on the CTB rims. As observed in ^{129}Xe-NMR spectra, the host molecules **105** and **106** showed weak binding to Xe in comparison with **102**. X-ray crystal structures of the complexes Xe@**105** and Xe@**106** showed very close Xe-arene intermolecular contacts and very high packing coefficients of 0.82 and 0.79, respectively.

3.2. Dynamic covalent synthesis

Hardie and co-workers have described a self-assembly strategy to afford cryptophanes and other cavitands.[67] One of the approaches in the self-assembly strategy is dynamic covalent synthesis, the generation of molecular hosts from functionalized precursors able to react under thermodynamic control by forming reversible covalent bonds and which can be promoted by the presence of template guest molecules resulting in the formation of the most stable host-guest complex. This approach has been used to obtain enantiopure CTB precursors.

In 2013, Cao, Chow and Kuck *et al.* reported an example of how CTB-like trimers can be employed to obtain cryptophanes *via* the self-assembly of the C_3-symmetrical tribenzotriquinacene (TBTQ)-trialdehyde (Scheme 17).[68] It involves a dynamic covalent synthesis of a mixture of three diastereomeric cryptophanes (94% yield) by stirring the racemic TBTQ-trialdehyde **108** and enantiomerically pure (1*S*,2*S*)-diaminocyclohexane **110** in CH_2Cl_2 at RT for 12 h (Scheme 18). All the three diastereomers (+)-(*P,P,S,S,S*) **111**, (+)-(*P,M,S,S,S*) **112** and (−)-(*M,M,S,S,S*) **113** can be separated by chromatography and further hydrolysis of (+)-(*P,P,S,S,S*) and (−)-(*M,M,S,S,S*) isomers in aqueous TFA afforded enantiomerically pure TBTQ-trialdehydes.

Warmuth *et al.* reported a similar approach to synthesize chiral (*P,P*) cryptophane (**116**, 92% yield) formed by heating racemic C_3 symmetric triformyl-CTB **114** and two equivalents of (1*R*,2*R*)-diaminocyclohexane (**115**, Scheme 18a).[69] The same group reported the dynamic covalent formation of cryptophane

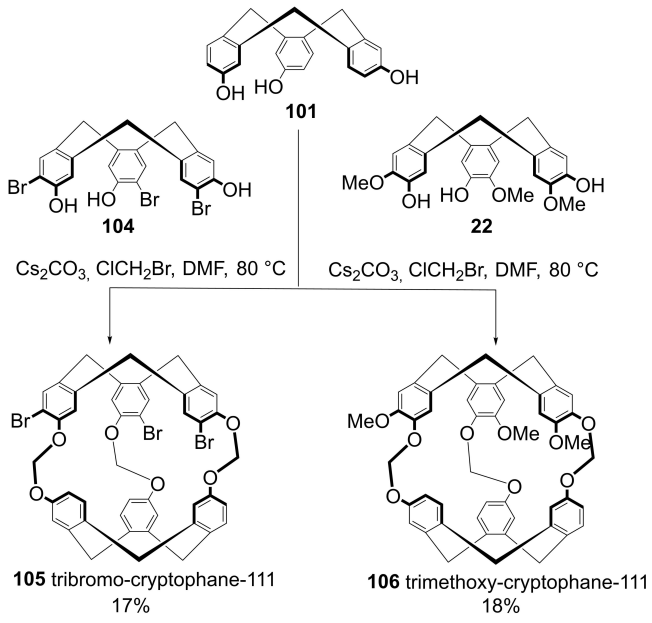

Scheme 16. Synthesis of Br_3-cryptophane-111 and $(MeO)_3$-cryptophane-111.

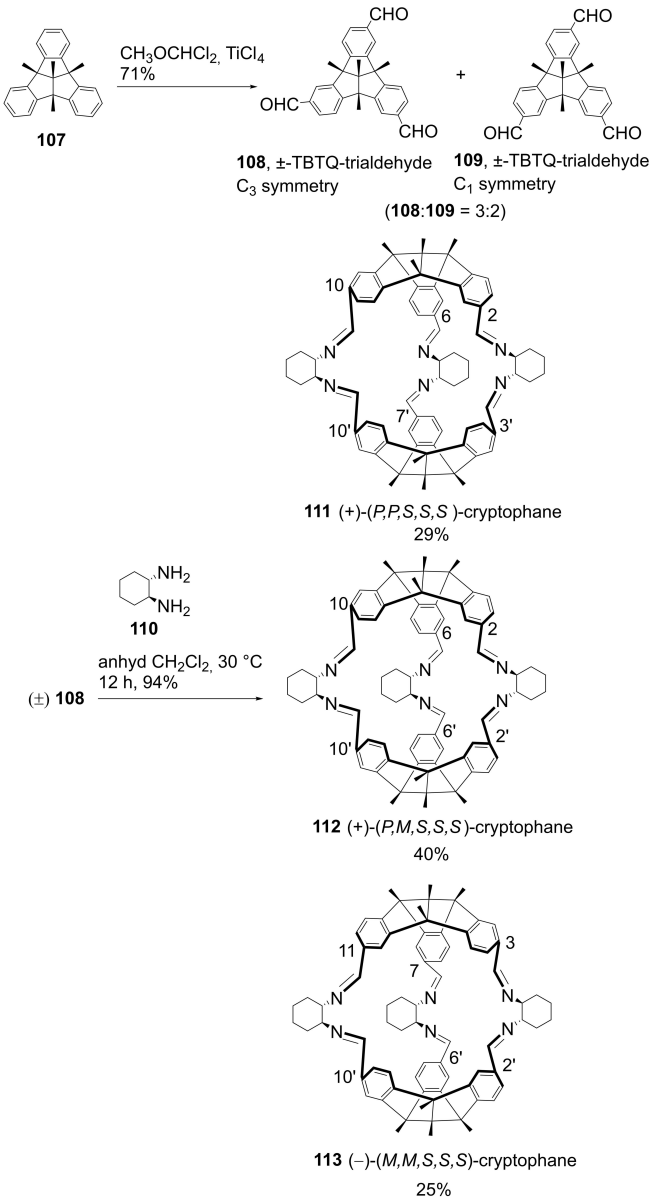

Scheme 17. Synthesis of Schiff-base containing cryptophanes from C_3-symmetrical TBTQ-trialdehyde.

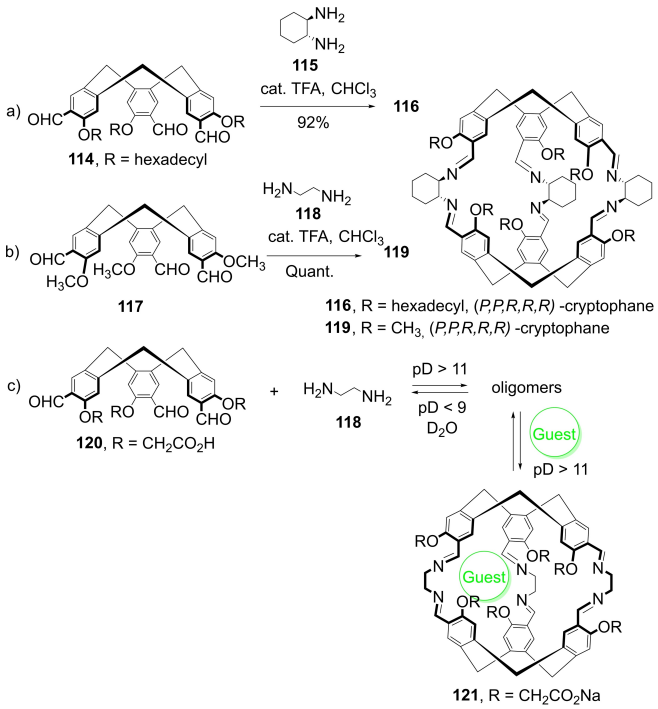

Scheme 18. Dynamic covalent synthesis of cryptophane, (a) and (b) mediated by TFA, (c) directed by a guest molecule.

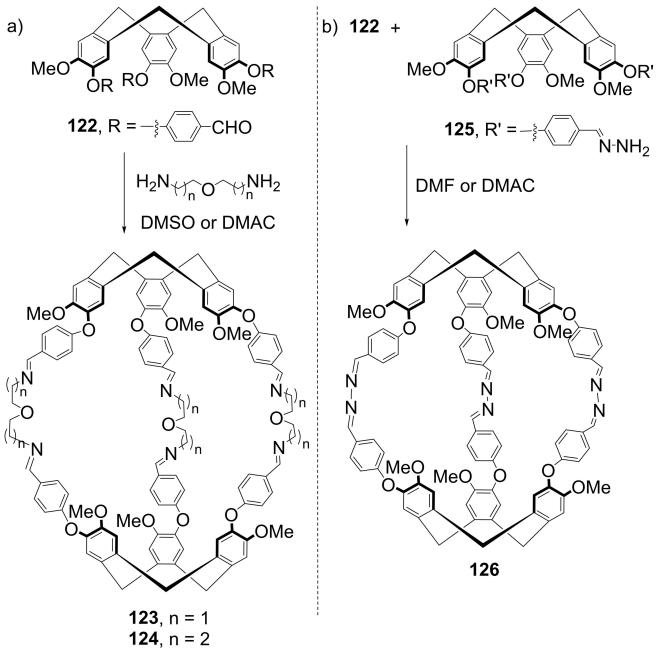

Scheme 19. Dynamic covalent synthesis of (a) imploded cryptophane (b) globular cryptophane.

in water.[70] Firstly in continuation to their previous work, **115** was replaced with 1,2-ethylene diamine (**118**, Scheme 18b), which still afforded racemic (*P,P*)/(*M,M*)-cryptophane **119** quantitatively. X-ray crystallography of **119** (crystallized from CH_2Cl_2/CH_3OH) showed a perfect CH−π interaction of a CH_2Cl_2 guest molecule with the aryl rings. This observation led to the hypothesis of spontaneous formation of cryptophane complex **121** from CTB **120** in the presence of **118** in D_2O at pD $>$11 by addition of traces of templating guest molecules $N(CH_3)_4OH$ or CH_2Cl_2 (Scheme 18c). Both the guest molecules resulted in spontaneous formation of **121** in approximately quantitative yields after about 2 hours. The stability of the complexes was dependent on pD with 12.5 being the optimal. In the absence or evaporation of guest molecules or presence of oversized templating guests, cryptophane got rearranged into oligomeric aggregates supporting the reversibility of the complex formation.

Hardie and coworkers synthesized cryptophanes (Scheme 19), whose crystal structures showed imploded *out – in* conformation from (±)-tris(4-formyl-phenyl)-cyclotriguaiacylene (**122**).[15b] The CTB **122** upon reaction with slight excess of bisoxydi(ethylamine) or bis(aminopropyl)ether formed *syn* cryptophane **123** and **124** respectively. Similar to the above discussed examples, cryptophanes were generated by imine bond formation, albeit without guest molecules in the cavity. Refluxing the cryptophanes **123** and **124** in DMSO for a short time showed in ^{1}H-NMR the initial major product as the *out – out* conformer along with a minor compound, which could be the intermediate *out – saddle* conformer. The *out – in* conformer reformed slowly and became dominant over 2 weeks for **123**. In case of **124**, the conformational changes occurred at notably slower rate and the solution did not reach equilibrium even after 36 days. A cryptophane **126** with shorter and rigid linkers was made from **122** and (±)tris-(4-benzaldehydehydrazone)-cyclotriguaiacylene (**125**). The crystal structure of **126** has three different cryptophanes in the asymmetric unit (differences in bond rotations of linkers or methoxy groups), however, all of them were *anti* isomers in *out – out* conformations with two molecules of dimethylacetamide (DMAC) in the cavities.

Cryptophanes containing the methylthio-substituents on the aromatic rim have been made by both the direct and template methods.[39] However, the coupling approach gave access to cryptophanes containing disulfide linkers. The smallest cryptophane-000 containing the two CTB units joined by disulfide links was first reported by Hardie and co-workers in 2012 (Scheme 20).[71] The first step involves the transformation of CTP **101** and CTG **22** to *O*-aryl *N,N*-dimethylthiocarbamate derivatives **128** and **129** in excellent 90% and 92% yields, respectively. A Newman-Kwart rearrangement at high temperatures to obtain *S*-aryl *N,N*-dimethylthiocarbamate derivatives **130** and **131**, and subsequent cleavage of thiocarbamate groups in the presence of base afforded cyclotrithiophenolenes **132** and **133**.[72] The precursor **132** underwent dimerization at ambient conditions. *Anti-S*-cryptophane-000 **134**, with the smallest cavity known so far, was isolated in 21% yield. Upon scale-up, traces of the *syn* isomer were also observed but it was inseparable from the major product. ^{1}H-NMR shows that **134** reversibly binds with methane in CD_2Cl_2 or $CDCl_3$ solution. The *syn-S*-cryptophane-000 also displayed a similar reversible binding pattern with nitrogen. Dimerization of trithio-CTG **133**, however, was not successful resulting in the formation of polymeric disulfide products.

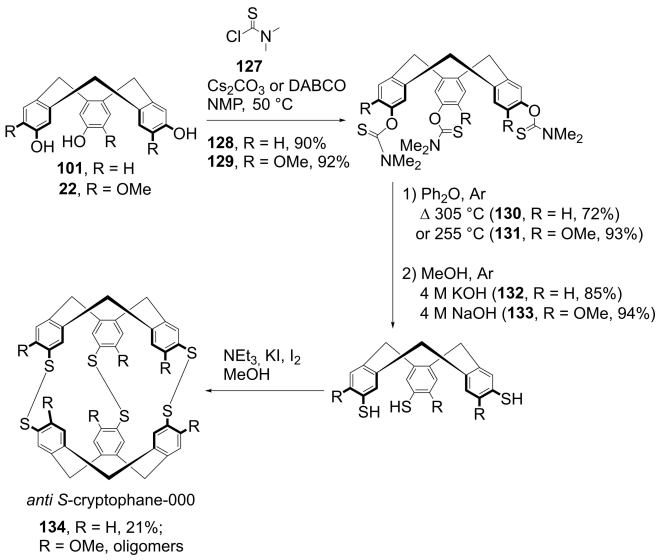

Scheme 20. Synthesis of cyclotrithiophenolenes and *S*-cryptophane-000.

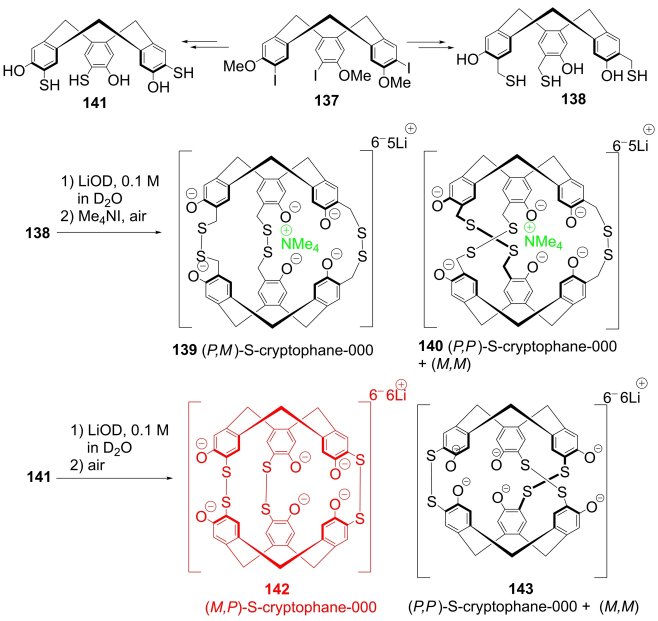

Scheme 22. Dynamic covalent synthesis of *S*-cryptophane-000.

To explain the possible steric clash between *ortho* methoxy-groups at the upper rim of approaching trithio-CTB molecules **133**, an offset cryptophane with bis(disulfide)-linkages was synthesized.[73] For this, a dithiol CTB precursor **135** was made from an incomplete Newman-Kwart rearrangement and deprotection (Scheme 21). The dimerization of the dithiol cavitand **135** resulted in the formation of one main product **136**. ^{1}H-NMR studies indicated a symmetric product but with three OMe signals at 3.80, 3.88 and 0.95 ppm. The upfield shift of one OMe signal could be possible if it is directed into the bowl of other cavitand, which was also confirmed by X-ray crystallography. Thus, the formation of offset cryptophane-like dimer **136** explains the observed oligomeric products in the dimerization of **133**.

Chambron, Aubert and co-workers have reported the synthesis of two different tris(disulphide)-linked cryptophanes in water (Scheme 22).[74] For this study, two mercapto-precursors were synthesized which differed in attachment of the thiol functional groups to the CTB core, such as with a methylene spacer in **138** and without the methylene spacer in **141**. The cyclotris(2-mercaptomethyl)phenolene **138**, with a methylene spacer, has three phenolic and three benzylic thio-groups with respective pK_a values of ca. 10.5 and 9.4, while the cyclotrimercaptophenolene precursor **141**, without the methylene spacer, has the respective pK_a values of 9.4 and 6.6 for the three phenolic and three thiophenolic groups. Dimerization experiments were conducted in the absence as well as presence of Me_4NI by dissolving **138** and **141** separately in deaerated 0.1 M LiOD in D_2O, while following the starting material conversion by ^{1}H-NMR. The solutions with the respective mercapto-precursors were incubated at 30 °C under atmospheric conditions for 2–3 days, resulting in the formation of cryptophane. The mercaptomethyl-precursor **138** resulted in the formation of a diastereomeric mixture of *anti-* and *meso-syn* forms containing Me_4N^+ cations. On the other hand, the mercapto-precursor **141** led to the formation of a diastereoselective single C_3-symmetric cryptophane **143** without template cations, presumably the *anti*-pair. The combinatorial experiments further proved that for the formation of cryptophane from the more rigid **141** does not require any template, unlike its flexible counterpart **138**. Additionally, the presence of larger cationic bases like 0.1 M CsOH, inhibited the cryptophane formation in **141**.

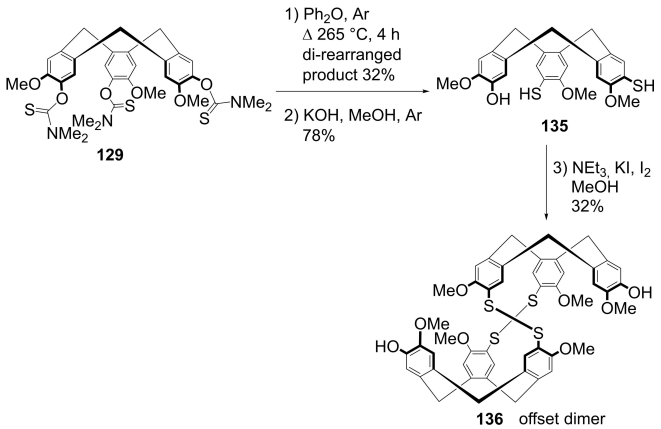

Scheme 21. Synthesis of offset dimer from dithiol-CTB.

3.3. Metal-ligand coordination

Metallo-cryptophanes have tripodal CTB ligands joined by metal-ligand coordination bonds giving a trigonal bipyramidal cage. After Zhong *et al.* reported the metal coordination approach to synthesize a mixture of *syn-* and *anti-* metallo-cryptophanes containing six Pd-ligand (CTB) bonds,[75] Hardie and co-workers published similar M_3L_2 examples with monodentate pyrimidine CTB ligands bearing *meta* N-donors.[76] The

tris[4-(5-pyrimidyl)benzoyl]-CTB was reacted with $[Ag(CH_3CN)_4]$ or with $Cu(NO_3)_2$ to obtain isomorphic *anti*-metallo-cryptophanes (Scheme 23). The presence of coordinating N-atoms in the *meta*-position and steric effects can allow only *anti*-isomer formation. Similar M_3L_2 type cages with Cu, Ir, Pd, Pt metal centers were reported independently by Hardie *et al.*[77] and Chambron *et al.*[78].

4. Late-stage functionalization

Most of the syntheses of functionalized cryptophanes have been reported using the template method with pre-functionalized template intermediates. This is by far the most promising approach since the direct method is known to afford low yields and the coupling method is particularly sensitive to steric hindrance. However, the template method usually involves synthetic routes with several steps in addition to a range of functional group interconversions (FGI). FGIs have been used quite often to make cryptophanes water-soluble and to generate accessible functional groups for further LSF. For example, FGIs have been applied to cryptophane-A (**62**) to transform all six −OMe groups to $-OCH_2COOH$, to study the effect of chemical structure of water soluble cryptophanes on chiroptical and binding properties.[14b] Similarly, enantiopure cryptophanol-A derivative containing six hydroxy-groups has been synthesized from enantiopure **62**.[79] Another example is the synthesis of C_1-symmetric cryptophane-H *via* FGI of cryptophanol-A (mono-hydroxy cryptophane-A) to its triflate and subsequent reduction.[80]

When it comes to the synthesis of cryptophanes bearing specific large side groups or electron-withdrawing groups suitable for various applications, LSF would clearly be an exceptionally valuable strategy.[81] However, this area is still in its infancy and considerable developments must be made to access a broader range of functionalized cryptophanes and LSF methods suitable for these scaffolds. A major challenge is to access enantiopure cryptophane cores in adequate amounts. Methods that have been reported for the resolution of cryptophane enantiomers till date are; 1) chiral resolution[42]; 2) chiral HPLC[50] and; 3) using enantiopure CTB precursors or asymmetric transformations.[69] Another typical challenge is low or moderate solubility of cryptophanes in organic solvents, except in DMSO, dimethylformamide (DMF) and halogenated solvents. Finally, the high molecular symmetry leads to a statistical distribution of products from LSF approaches, potentially leading to low yields and complicated purification of the desired products. Some of these difficulties are evident in the chemistry described in this section.

Together with Holman, Brotin and Dutasta reported the late-stage metalation of **102** with six $[(\eta^5\text{-}C_5Me_5)Ru^{II}]^+$ in 89% yield (Scheme 24).[82] Excess of $[Cp^*Ru(\mu_3\text{-}Cl)]_4$ with **102** was microwave-irradiated in THF/H_2O under anaerobic conditions to afford the air-stable and water-soluble hexachloride salt **146**. The cryptophane **146**, is the first water-soluble derivative of **102**, and has Xe-binding constant $K_a = 2.9(2) \times 10^4\ M^{-1}$ at 293 K. However, the exact role of Ru in the thermodynamic affinity of Xe for **146** has not been studied. The presence of cationic, electron-withdrawing Ru moieties resulted in a large downfield change in the chemical shift of the Xe@**146** complex in comparison with the Xe@**102** complex. Rousseau *et al.* reported the first metal-free water-soluble cryptophane-111.[83] It is an example of post-synthetic derivatization of **102** where carboxylic acid functionalization[64] in **147** is transformed to tri-sulfonated linker in **149** *via* amide coupling in the presence of peptide coupling reagent benzotriazol-1-yloxytripyrrolidinophosphonium hexafluorophosphate (PyBOP) (Scheme 24). ^{129}Xe-NMR experiments showed the Xe in-out exchange rate for the Xe@**149** complex to be higher than 20 Hz, which is interesting for future imaging studies. Additionally, the ^{129}Xe-NMR spectrum of the Xe@**149** complex in D_2O displayed a wide chemical shift difference of 2.6 ppm between signals corresponding to two diastereomeric complexes because of a single chiral center located in the tri-sulfonated linker.

The previously reported NBS-mediated monobromination[64] was explored further, and treating **102** with excess reagent for 13 days at ambient temperature afforded the hexabrominated core **150** in 60% yield (Scheme 25).[84] **150** was subjected to lithium-halogen exchange and subsequently quenched with CO_2 with the aim of obtaining the corresponding water-soluble hexacarboxylic acid. However, at −78 °C most of the **150** was

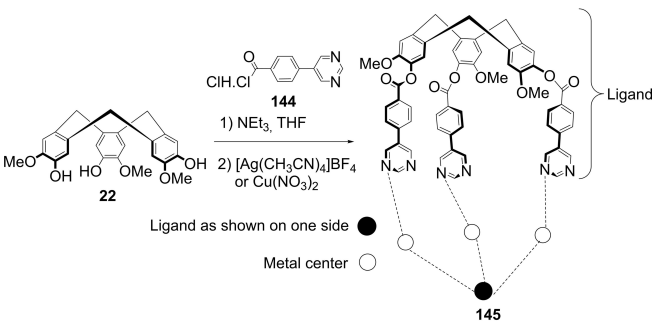

Scheme 23. Synthesis of metallo-cryptophanes through metal-ligand coordination.

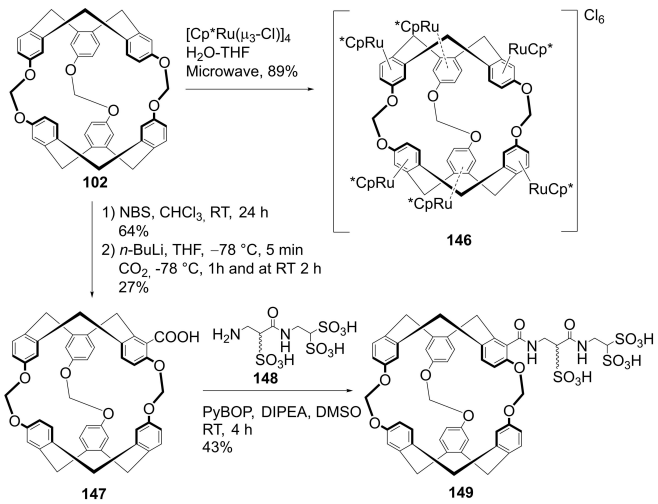

Scheme 24. LSF of Cryptophane-111.

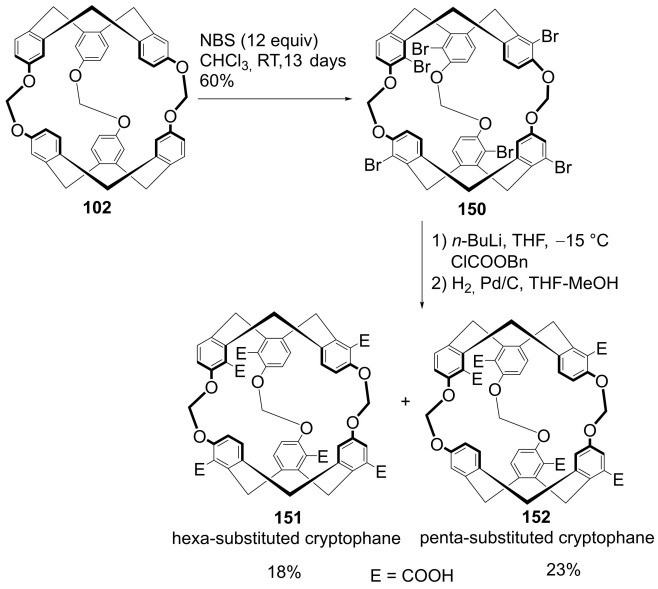

Scheme 25. Hexa-bromination of cryptophane-111 and its transformation to carboxylic acids.

recovered, while at −15 °C, all of the halogen positions were lithiated but it did not proceed to form the desired product. Despite increasing the temperature, only minor amounts of mono- and di-carboxylic acid compounds were formed. Switching to a more reactive electrophile, benzylchloroformate, resulted in a mixture of penta- and hexa-substitution. This mixture was subjected to hydrogenolysis to isolate hexacarboxylic acid **151** in 18% overall yield and the penta-substituted derivative **152** in 23% overall yield from **150**.

There are several examples of cryptophane-A derived biosensors reported in the last decade, among which the majority are mono-functionalized derivatives and some of them are discussed below.[18a,34,85]

Berthault and Rousseau reported functionalization of racemic as well as enantiopure hexacarboxylic acid cryptophane-A (**153**) to detect Zn^{2+} ions by ^{129}Xe-NMR spectroscopy (Scheme 26).[86] A single carboxylic acid was activated by esterification with *N*-hydroxysuccinimide (NHS) followed by coupling with a primary amine attached through a spacer to

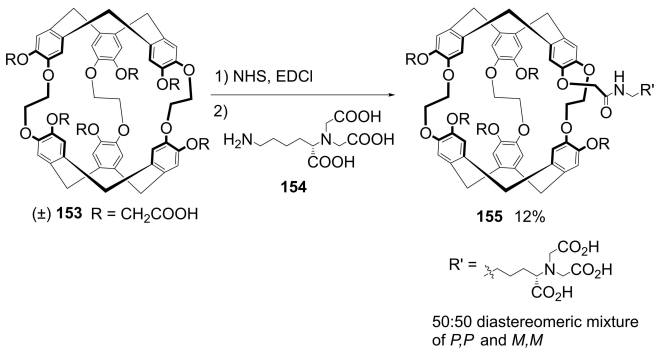

Scheme 26. Synthesis of NTA-functionalized pentacarboxylic acid cryptophane-A.

the zinc chelating nitrilotriacetic acid (NTA) moiety (**154**) to obtain monofunctionalized cryptophane **155**. In the absence of Zn^{2+} ions ^{129}Xe-NMR spectrum at 293 K showed two signals, one at 196 ppm for free Xe in water and second at 65.6 ppm for the Xe@**155** complex. Interestingly, in the presence of Zn^{2+} ions, the second signal was split into two new signals at 65.75 ppm and 67.2 ppm. This variation is attributed to the chelation of Zn^{2+} ions with the NTA moiety as it causes a change in the electron density experienced by the caged Xe-guest molecule. Additionally, chelation also reduces the flexibility of the spacer, thereby allowing the diastereomeric mixture **155** to give two separate signals. The observation was supported by the ^{129}Xe-NMR spectrum of diastereomerically pure Xe@**155** complex showing only one signal.

The same group reported the functionalization of enantiopure hexacarboxylic acid cryptophane **153** with fluorescent biarsenical probes CrAsH for the detection of tetracysteine (Cys4) tagged proteins (Figure 4).[87] The two enantiomers (*M,M*)-**153** and (*P,P*)-**153** were synthesized from enantiopure cryptophanol-A.[14b] The (*M,M*)-**153** was covalently bonded to two CrAsH derivatives (from an equimolar mixture of 5-carboxyfluorescein and 6-carboxyfluorescein) through an amide linkage, affording two regioisomers *(M,M)*-**156a** and *(M,M)*-**156b** separated by HPLC in 15% and 9% yields respectively. In the presence of Cys4 tagged peptide, the biosensor *(M,M)*-**156a** showed strong fluorescence signal plus different ^{129}Xe-NMR signals for caged Xe and free biosensor. The study has been optimized further by investigating both the regioisomers of (*M,M*)-**156** and (*P,P*)-**156a** with three tagged peptide motifs.[88] The biosensor (*P,P*)-**156b** was impossible to isolate from the other regioisomer due to low yield of the reaction. Among all

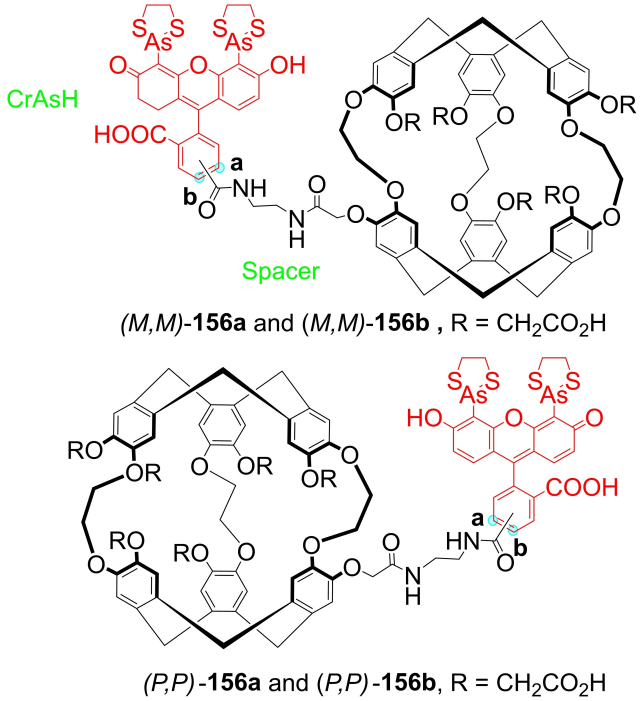

Figure 4. Synthesis of CrAsH-functionalized pentacarboxylic acid cryptophane-A for the *in vitro* detection of proteins.

the combinations of the biosensors and tagged peptide motifs, the combination of *(P,P)*-**156a** with the third flexible strand peptide was the most efficient in terms of ^{129}Xe-NMR and fluorescence signals.

Rousseau, Berthault, Rivera and coworkers reported the mono-functionalization of racemic **153** with a peptide-amine linker chain, to generate a bimodal probe **157** targeting Epidermal Growth Factor Receptors (EGFR) overexpressed in cancer cells (Figure 5).[89] The peptide moiety comprises of three amino acid units: one lysine bearing fluorescein group (5-FAM) for fluorescence spectroscopy, another lysine containing primary amine side chain to attach to cryptophane *via* an amide linkage and a cysteine providing a thiol functionality. A single carboxylic acid on cryptophane **153** is activated and attached to the peptide moiety to give a mixture of diastereomers in 13% isolated yield. The thiol functionality is bio-conjugated to cetuximab (therapeutic antibody) through thiol-maleimide addition to generate the biosensor **157**. The biosensor **157** showed high selectivity towards the receptors and the biological activity was similar to the antibody as observed in flow cytometry and immunofluorescence studies. HyperCEST ^{129}Xe-NMR was successful in detecting **157** in human cell lines.

Schröder and Hennig have disclosed the synthesis of two cryptophanes conjugated with near-infrared (NIR) fluorescent dyes DY680 and DY682, generated from the cryptophane A monoacid **158**.[90] Cryptophane **158** was first converted to the terminal linker amine before coupling with NHS ester-forms of the dyes in the presence of phosphate buffers as shown in Scheme 27. The incorporation of these cryptophane conjugates **159** and **160** into giant unilamellar vesicles and uniformly sized large unilamellar vesicles (biomembrane models) of varying phospholipid composition was studied by fluorescence spectroscopy and Hyper-CEST NMR.

The group has also functionalized **158** through peptide coupling with PEGylated fluorescein (PEG-FAM).[91] The product **161** was generated in 50% overall yield in six steps, starting from the synthesis of PEG-FAM building block and followed by the coupling of **158**. In another experiment, **158** was coupled with PEGylated tetramethylrhodamine (PEG-TAMRA) by microwave-assisted peptide coupling and product **162** was isolated in 45% overall yield starting from the synthesis of PEG-TAMRA building block and including the coupling of **158** (Figure 6). The bioconjugate **162** showed higher levels of cellular uptake and consequently lower percentage of cell viability in comparison to **161**. Nevertheless, NMR and optical imaging studies demonstrated both as suitable candidates for MRI-based cell labelling.

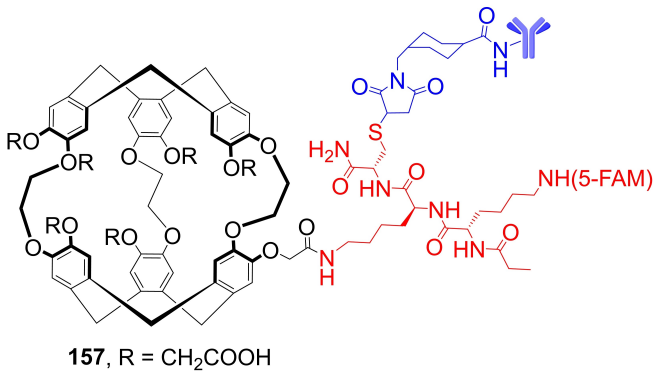

Figure 5. Synthesis of EGFR targeting bimodal probe from cryptophane.

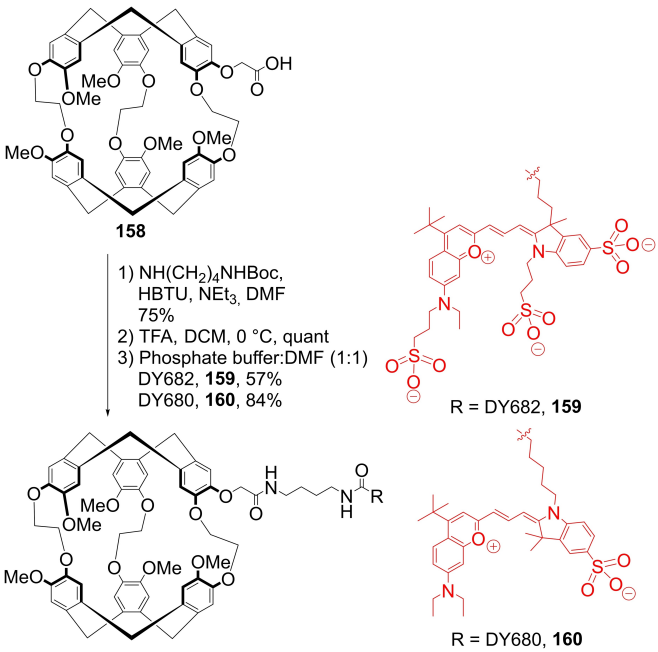

Scheme 27. LSF of cryptophane-A monoacid to generate cryptophane-fluorescent dye conjugates.

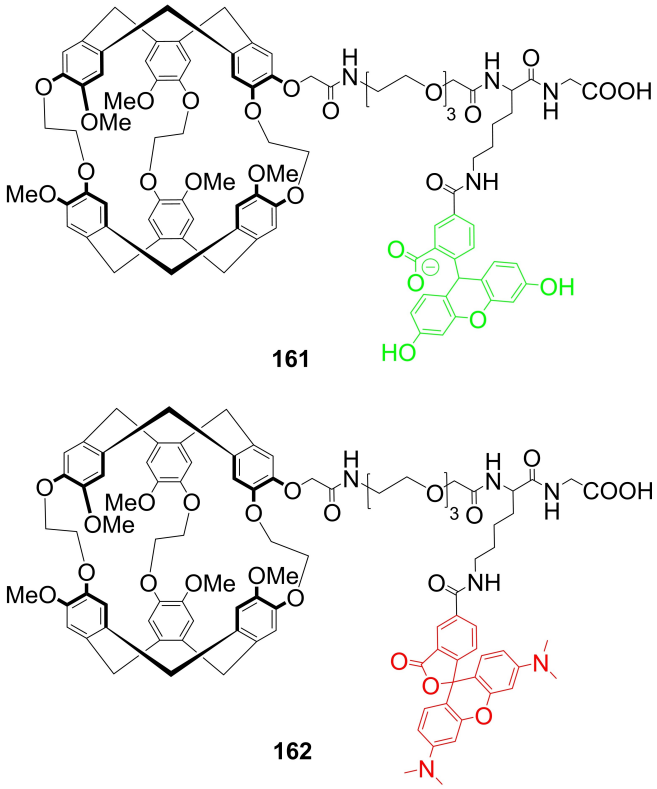

Figure 6. Examples of cryptophane-A biosensors, cryptophane-A-PEG-FAM (**161**) and cryptophane-A-PEG-TAMRA (**162**).

Additionally, the free carboxylic terminus in **161** and **162** can be easily activated for further functionalization. The functionalized cryptophane **161** was used in cell tracking studies.[92] Another study reported functionalization of a cryptophane-A-diacid with hydrophilic dendrimers to generate very bulky and water soluble conjugates.[93] Schröder *et al.* also reported a complete synthesis of a ^{129}Xe-biosensor on solid support starting from cryptophane-A-diacid.[94]

Buffeteau *et al.* reported the grafting of cryptophane derivatives prepared from cryptophanol-A onto gold and silica (SiO_2/Au) surfaces (Figure 7).[95] Polarization modulation infrared reflection-absorption spectroscopy (PM-IRRAS) was used to characterize all the cryptophane-derived self-assembled monolayers (SAM) **163** – **166**. In this study, SAM of cryptophanol-A derivative bearing decanethiol chain **163** were prepared by dipping Au substrates in THF solution of the cryptophane decanethiol derivative for 24 h. The surface coverage was nearly 100% for cryptophane decanethiol derivative **163**. A cysteamine derivative of cryptophanol-A was also grafted onto Au (**164**) and the surface coverage was 75%. To immobilize monocarboxylic acid and hexa-carboxylic acid derivatives of cryptophane-A on to a silica surface, amino-terminated SAMs were grafted first by silanization. Amide bond formation between the amino-terminated SAM and activated carboxylic acid of cryptophane-A derivatives in DMF or CH_2Cl_2 solution resulted in immobilization of the cryptophane on silica (**165** and **166**).

Zhou and coworkers reported the synthesis of a molecular clamp **167** consisting of a dipyrrolylquinoxaline (DPQ) derivative with two cryptophane-A moieties for the detection of Hg^{2+} ions (Figure 8).[96] The cryptophane-A hydrazine was synthesized from cryptophanol-A and 2,3-bis(5-formylpyrrol-2-yl)-quinoxaline to obtain the chemosensor in 86% yield. The pyrrole and the imine parts of the sensor **167** serve as the recognition site for the Hg^{2+}. UV absorbance intensity showed the chemosensor to be ion-selective. ^{129}Xe-NMR of Xe@**167** showed an upfield shift in the presence of Hg^{2+}. The binding mechanism was deduced by NOESY experiments conducted in the absence and presence of Hg^{2+}.

The same group also reported a molecular sensor for the detection and imaging of hydrogen sulfide (Figure 9a).[33b] Racemic **158** was coupled with *N*-ethylamino-4-azido-1,8-naphthalic anhydride to obtain the sensor **168** in 63% yield. In the presence of H_2S, the azide group undergoes reduction to amine and a strong green fluorescence can be observed.[97] ^{129}Xe-NMR displayed a chemical shift difference of 1.1 ppm for the encapsulated Xe in the absence versus presence of H_2S. The sensor **168** was observed to be selective for H_2S and suitable for imaging in living cells.

For *in vitro* detection of biothiols, such as cysteine (Cys), homocysteine (Hcy) and glutathione (GSH), Zhou *et. al.* reported a biosensor **169** derived from acrylation of racemic cryptophanol-A (Figure 9b).[98] In the presence of biothiols, the acrylate group undergoes a thiol-addition reaction to form thioether, which was observed by TOF-MS and ^{1}H-NMR experiments. ^{129}Xe-NMR spectra of Xe@**169** showed an upfield chemical shift change of 1.4 ppm for caged Xe in the presence of Cys and upfield shift of 1.2 ppm in the presence of Hcy and GSH. The characteristic feature of **169** to differentiate Cys from Hcy and GSH was also tested in bovine serum solution. Progressing further towards the *in vivo* detection of biothiols targeting mitochondria, the group reported a new biosensor **170** derived

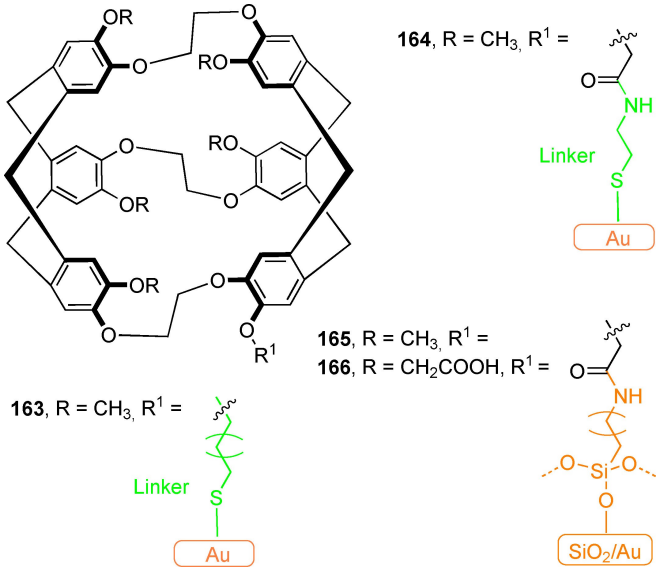

Figure 7. Cryptophane-222 derivatives grafted onto Au and SiO_2/Au surfaces.

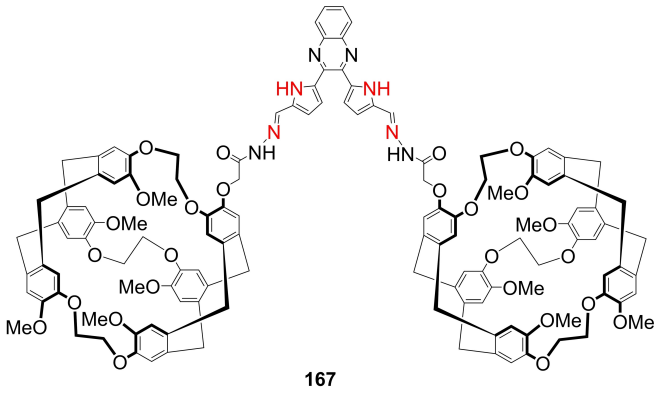

Figure 8. Molecular sensor for the detection of mercury ions.

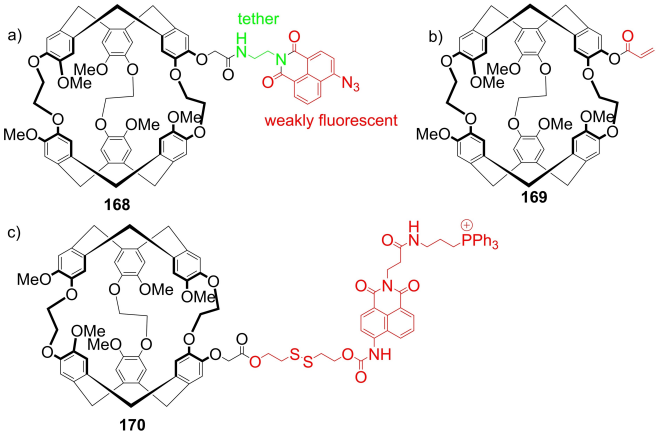

Figure 9. Molecular sensors for the detection of *S*-containing compounds.

from **158** coupled to a large side group containing disulfide (linker), naphthalimide (fluorescence group),and triphenylphosphonium (targeting group) moieties (Figure 9c).[99] Compared to the previous biosensor **169** (10 μM), **170** has lower detection limit (0.1 nM) and the fluorescence intensity was enhanced upon reacting with biothiol. It is selective for biothiols and stable across a broad pH range. ^{129}Xe-NMR showed an upfield shift of 1.4 ppm for caged Xe in the presence of GSH, Cys, and Hcy. Cellular hyper-CEST ^{129}Xe-NMR and cellular fluorescence imaging experiments demonstrated the applicability of **170** in cell studies.

Zhou's group also reported a porphyrin-functionalized cryptophane-A derivative **171** as a small multifunctional tool (SMFT) for pH detection, fluorescence imaging suitable for cells as well as tumors *in vivo* and photodynamic therapy (PDT) (Figure 10).[100] Hyper-CEST ^{129}Xe-NMR experiments showed that the^{129}Xe signal intensity increased with pH. The SMFT **171** was tested on a tumor model of nude mice as a fluorescent probe for animal imaging and was found to be primarily localized in the tumor. It showed good efficiency in the production of singlet oxygen in buffers (pH 4 and 8).

To make the cryptophane-based biosensor suitable for molecular imaging of cancer cells, Pines and Francis incorporated mono-functionalized cryptophane-A in filamentous fd bacteriophage that can recognize the EGF receptor with high specificity.[85b] Another example of functionalized cryptophane-A coupled to a tris(trifluoromethyl) containing large side group, was incorporated in designing nanoemulsions for the development of novel theranostics.[101] The nanoemulsion structure also contains fluorinated dendron and tetrabenzylporphyrin components to enhance Hyper-CEST ^{129}Xe MRI, ^{19}F MRI and fluorescence imaging signals. It facilitated selective detection of integrin $\alpha_v\beta_3$ overexpressed in cancer cells along with multiple imaging functions and efficient PDT.

Dmochowski *et al.* reported the functionalization of tripropargyl cryptophane **6a** with 2-azidoethylamine *via* a Cu(I)-catalyzed [3 + 2] azide-alkyne cycloaddition (CuAAC) reaction to obtain water-soluble tris-(triazoleethylamine) cryptophane (TTEC, **172**, Figure 11) to measure Xe and Ra association constants as Xe@**172** $K_a = 42{,}000 \pm 2{,}000\ M^{-1}$at 293 K and Ra@**172** $K_a = 49{,}000 \pm 12{,}000\ M^{-1}$at 293 K by isothermal titration calorimetry and radiometric methods respectively.[18b] The same group has also functionalized monopropargyl cryptophane-A with the *N*-terminal azide of a peptide-folate conjugate via

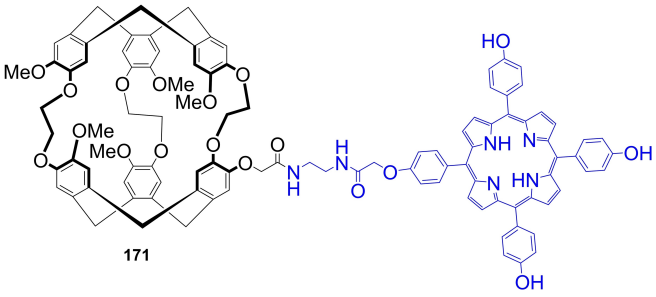

171

Figure 10. Cryptophane-A derived SMFT.

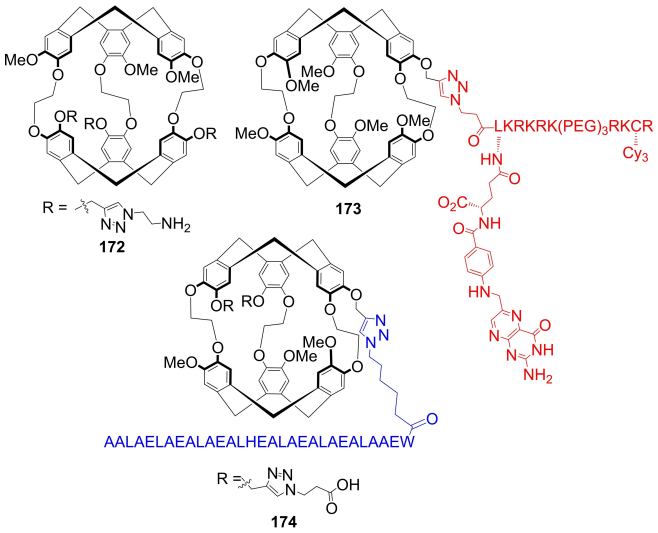

Figure 11. Examples of functionalized cryptophane-A derivatives.

CuAAC, followed by the attachment of a cyanine Cy3 fluorescent dye to the peptide moiety to afford cryptophane A-biosensor **173** (Figure 11).[33a] The convergent synthetic route comprises of overall 20 steps. The biosensor was aimed to target membrane-bound folate receptors. At low micromolar concentrations **173** was observed to be non-toxic in HT-1080 and KB cells. ^{129}Xe-NMR, cellular internalization and competitive blocking experiments were also conducted. In another report, racemic **6a** was functionalized with an EALA-oligopeptide and 3-azidopropionic acid (water solubilizing group) via two subsequent CuAAC reactions, to make a ^{129}Xe-NMR biosensor **174** for labelling cells in acidic microenvironment (Figure 11).[102] The characteristic feature of 30mer EALA- oligopeptide is, at pH 7.5 the peptide has a disordered conformation, while at pH 5.5 is α-helical and becomes capable of inserting into lipophilic membrane. This characteristic feature was retained by the peptide even after it was attached to the cryptophane. In cellular hyper-CEST ^{129}Xe-NMR studies, the chemical shift showed a 13.4 ppm downfield shift for membrane inserted Xe@**174** complex at pH 5.5 with respect to Xe@**174** complex in cell solution at pH 7.5.

Two enantiopure isomers of tripropargyl cryptophane **6a** were separately mono-functionalized with 4-(azidomethyl)benzenesulfonamide and subsequently subjected to CuAAC reaction to attach benzenesulfonamide moiety separated by a 7-bond linker, to target carbonic anhydrase-II (CA-II).[103] Another subsequent CuAAC reaction with excess 3-azidopropionic acid afforded water-soluble enantiomeric tri-functionalized cryptophane-A biosensors **175** and **176** (Figure 12). Hyperpolarized ^{129}Xe-spectroscopy of these single enantiomers complexed with CA-II showed two bound Xe signals at 72 and 68 ppm for Xe@(−)**175** and 68 and 67 ppm for Xe@(+)**176**. These results were also supported by X-ray crystallography, showing both cryptophane biosensors **175** and **176** bind with CA-II at Zn^{2+} active site and another site near the protein surface.

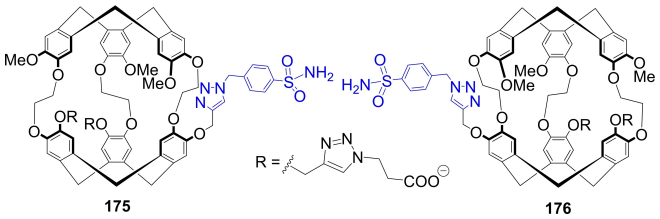

Figure 12. Examples of tri-functionalized cryptophane-A biosensors (−) **175** and (+) **176** cryptophane benzenesulfonamide derivatives.

5. Conclusions

This review has discussed recent advances in the synthesis of functionalized cryptophanes. The main synthetic strategies are still in use, but the template method appears to be the generally most versatile and successful approach in the past decade. The coupling approach via bimolecular nucleophilic substitution is advantageous for the synthesis of unsubstituted cryptophanes. For substituted CTBs, steric interactions between the rim-substituents are a limiting factor. However, self-assembly approaches have given comparatively better results even in the presence of proximal substituents. In any method, the production of the cryptophane core skeleton is a multi-step synthesis. Late-stage functionalization of these compounds is the ideal approach to obtain functionalized systems, particularly when considering the challenges of generating the skeletal structures in practical yields. Some progress has been made in functionalization of cryptophane-111, although most examples so far are described for the cryptophane-A scaffold. Consequently, functionalized cryptophanes with better solubilizing functional groups have been reported.

Despite the many recent advances described in this review article, major challenges remain to be met in the field of cryptophane synthesis. One of these is the preparation of cryptophanes in larger quantities. This review clearly demonstrates the complexity involved in many systems and low chemical yields are quite common. For instance, the introduction of electron-withdrawing substituents onto cryptophane scaffolds has turned out to be a considerable task that can only be addressed by late-stage functionalization strategies and is an important future challenge. Moreover, although some progress has been described herein, the majority of studies are concerned with *anti*-cryptophanes, thus the efficient generation of *syn*-cryptophanes is another future direction in the field and includes methods for accessing the enantiopure forms of the various isomers. The expanding needs and applications of designer-cryptophanes, particularly in a range of emerging molecular sensor technologies, suggests that cryptophanes represent a frontier challenge for late-stage functionalization.

Acknowledgements

The authors wish to acknowledge support for this project from the Research Council of Norway (JHH, Grant no. 275043 CasCat) and the Faculty of Natural Sciences and Technology at UiT The Arctic University of Norway (SK, JHH).

Conflict of Interests

The authors declare no conflict of interest.

Data Availability Statement

Data sharing is not applicable to this article as no new data were created or analyzed in this study.

Keywords: cryptophane · cyclotriveratrylenes · supramolecular hosts · cage molecules · late-stage functionalizations

[1] The Nobel Prize in Chemistry **1987**, Nobel Prize Outreach AB.
[2] G. Crini, *Chem. Rev.* **2014**, *114*, 10940–10975.
[3] C. D. Gutsche, *Calixarenes: an introduction*, Royal Society of Chemistry, **2008**.
[4] S. J. Barrow, S. Kasera, M. J. Rowland, J. Del Barrio, O. A. Scherman, *Chem. Rev.* **2015**, *115*, 12320–12406.
[5] F. Nicoli, M. Baroncini, S. Silvi, J. Groppi, A. Credi, *Org. Chem. Front.* **2021**, *8*, 5531–5549.
[6] C. M. Zaleski, *Advances in metallacrown chemistry*, Springer Nature, **2022**.
[7] M. Zhang, X. Yan, F. Huang, Z. Niu, H. W. Gibson, *Acc. Chem. Res.* **2014**, *47*, 1995–2005.
[8] M. Xue, Y. Yang, X. Chi, Z. Zhang, F. Huang, *Acc. Chem. Res.* **2012**, *45*, 1294–1308.
[9] J. Murray, K. Kim, T. Ogoshi, W. Yao, B. C. Gibb, *Chem. Soc. Rev.* **2017**, *46*, 2479–2496.
[10] I. Roy, A. H. G. David, P. J. Das, D. J. Pe, J. F. Stoddart, *Chem. Soc. Rev.* **2022**, *51*, 5557–5605.
[11] J. Gabard, A. Collet, *J. Chem. Soc. Chem. Commun.* **1981**, 1137–1139.
[12] O. Baydoun, T. Buffeteau, T. Brotin, *Chirality* **2021**, *33*, 562–596.
[13] A. Collet, *Tetrahedron* **1987**, *43*, 5725–5759.
[14] a) O. Taratula, P. A. Hill, N. S. Khan, P. J. Carroll, I. J. Dmochowski, *Nat. Commun.* **2010**, *1*, 148; b) A. Bouchet, T. Brotin, M. Linares, D. Cavagnat, T. Buffeteau, *J. Org. Chem.* **2011**, *76*, 7816–7825.
[15] a) P. Ghosh, M. Hossain, P. Saradhi Satha, C. Shekhar Purohit, *Chem. Asian J.* **2023**, *18*, e202300428; b) F. L. Thorp-Greenwood, M. J. Howard, L. T. Kuhn, M. J. Hardie, *Chem. Eur. J.* **2019**, *25*, 3536–3540.
[16] G. Huber, T. Brotin, L. Dubois, H. Desvaux, J.-P. Dutasta, P. Berthault, *J. Am. Chem. Soc.* **2006**, *128*, 6239–6246.
[17] M. Doll, P. Berthault, E. Léonce, C. Boutin, E. Jeanneau, T. Brotin, N. De Rycke, *J. Org. Chem.* **2022**, *87*, 2912–2920.
[18] a) S. D. Zemerov, I. J. Dmochowski, *RSC Adv.* **2021**, *11*, 7693–7703; b) D. R. Jacobson, N. S. Khan, R. Collé, R. Fitzgerald, L. Laureano-Pérez, Y. Bai, I. J. Dmochowski, *Proc. Nat. Acad. Sci.* **2011**, *108*, 10969–10973.
[19] K. E. Chaffee, H. A. Fogarty, T. Brotin, B. M. Goodson, J.-P. Dutasta, *J. Phys. Chem. A* **2009**, *113*, 13675–13684.
[20] H. A. Fogarty, P. Berthault, T. Brotin, G. Huber, H. Desvaux, J.-P. Dutasta, *J. Am. Chem. Soc.* **2007**, *129*, 10332–10333.
[21] a) J. Crassous, S. Hediger, *J. Phys. Chem. A* **2003**, *107*, 10233–10240; b) .Y. Shi, X. Li, J. Yang, F. Gao, C. Tao, *J. Fluoresc.* **2011**, *21*, 531–538.
[22] a) A. Bouchet, T. Brotin, M. Linares, H. Ågren, D. Cavagnat, T. Buffeteau, *J. Org. Chem.* **2011**, *76*, 4178–4181; b) N. De Rycke, M. Jean, N. Vanthuyne, T. Buffeteau, T. Brotin, *Eur. J. Org. Chem.* **2018**, *2018*, 1601–1607.
[23] D. J. Cram, M. E. Tanner, S. J. Keipert, C. B. Knobler, *J. Am. Chem. Soc.* **1991**, *113*, 8909–8916.
[24] L. Garel, B. Lozach, J. P. Dutasta, A. Collet, *J. Am. Chem. Soc.* **1993**, *115*, 11652–11653.
[25] T. Brotin, D. Cavagnat, P. Berthault, R. Montserret, T. Buffeteau, *J. Phys. Chem. B* **2012**, *116*, 10905–10914.
[26] a) R. M. Fairchild, K. T. Holman, *J. Am. Chem. Soc.* **2005**, *127*, 16364–16365; b) A. Collet, J.-P. Dutasta, B. Lozach, J. Canceill, in *Supramol.*

Chem. I — Directed Synthesis and Molecular Recognition (Eds.: J. Canceill, J. C. Chambron, A. Collet, C. Dietrich-Buchecker, H. D. Durst, J. P. Dutasta, F. H. Kohnke, B. Lozach, J. P. Mathias, S. Misumi, J. P. Sauvage, J. F. Stoddart, D. A. Tomalia, S. C. Zimmerman), Springer Berlin Heidelberg, Berlin, Heidelberg, **1993**, pp. 103–129.
[27] a) T. B. Demissie, K. Ruud, J. H. Hansen, *J. Phys. Chem. A* **2017**, *121*, 9669–9677; b) A. Bagno, G. Saielli, *Chem. Eur. J.* **2012**, *18*, 7341–7345.
[28] E. Dubost, J.-P. Dognon, B. Rousseau, G. Milanole, C. Dugave, Y. Boulard, E. Léonce, C. Boutin, P. Berthault, *Angew. Chem. Int. Ed.* **2014**, *53*, 9837–9840.
[29] L. Gao, W. Liu, O.-S. Lee, I. J. Dmochowski, J. G. Saven, *Chem. Sci.* **2015**, *6*, 7238–7248.
[30] a) P. Hilla, J. Vaara, *Phys. Chem. Chem. Phys.* **2022**, *24*, 17946–17950; b) P. Hilla, J. Vaara, *Phys. Chem. Chem. Phys.* **2023**, *25*, 22719–22733.
[31] K. V. J. Jose, D. Beckett, K. Raghavachari, *J. Chem. Theory Comput.* **2015**, *11*, 4238–4247.
[32] a) K. V. Jovan Jose, K. Raghavachari, *J. Chem. Theory Comput.* **2016**, *12*, 585–594; b) L. C. G. D'haese, N. Daugey, D. Pitrat, T. Brotin, J. Kapitán, V. Liégeois, *Spectrochim. Acta Part A* **2024**, *306*, 123484.
[33] a) N. S. Khan, B. A. Riggle, G. K. Seward, Y. Bai, I. J. Dmochowski, *Bioconjugate Chem.* **2015**, *26*, 101–109; b) S. Yang, Y. Yuan, W. Jiang, L. Ren, H. Deng, L. S. Bouchard, X. Zhou, M. Liu, *Chem. Eur. J.* **2017**, *23*, 7648–7652.
[34] H. M. Rose, C. Witte, F. Rossella, S. Klippel, C. Freund, L. Schröder, *Proc. Nat. Acad. Sci.* **2014**, *111*, 11697–11702.
[35] a) Y. Li, H. Li, C. Lin, *Tetrahedron Lett.* **2022**, *103*, 154007; b) L. Peyrard, S. Chierici, S. Pinet, P. Batat, G. Jonusauskas, N. Pinaud, P. Meyrand, I. Gosse, *Org. Biomol. Chem.* **2011**, *9*, 8489–8494.
[36] a) M.-J. Li, C.-C. Lai, Y.-H. Liu, S.-M. Peng, S.-H. Chiu, *Chem. Commun.* **2009**, 5814–5816; b) M.-J. Li, C.-H. Huang, C.-C. Lai, S.-H. Chiu, *Org. Lett.* **2012**, *14*, 6146–6149; c) M.-Y. Ku, S.-J. Huang, S.-L. Huang, Y.-H. Liu, C.-C. Lai, S.-M. Peng, S.-H. Chiu, *Chem. Commun.* **2014**, *50*, 11709–11712; d) K.-S. Liu, M.-J. Li, C.-C. Lai, S.-H. Chiu, *Chem. Eur. J.* **2016**, *22*, 17468–17476.
[37] G. El-Ayle, K. T. Holman, in *Comprehensive Supramol. Chem. II* (Ed.: J. L. Atwood), Elsevier, Oxford, **2017**, pp. 199–249.
[38] T. Brotin, J.-P. Dutasta, *Eur. J. Org. Chem.* **2003**, *2003*, 973–984.
[39] T. Brotin, J.-P. Dutasta, *Chem. Rev.* **2009**, *109*, 88–130.
[40] T. Brotin, V. Roy, J.-P. Dutasta, *J. Org. Chem.* **2005**, *70*, 6187–6195.
[41] O. Taratula, P. A. Hill, Y. Bai, N. S. Khan, I. J. Dmochowski, *Org. Lett.* **2011**, *13*, 1414–1417.
[42] O. Taratula, M. P. Kim, Y. Bai, J. P. Philbin, B. A. Riggle, D. N. Haase, I. J. Dmochowski, *Org. Lett.* **2012**, *14*, 3580–3583.
[43] L. Delacour, N. Kotera, T. Traoré, S. Garcia-Argote, C. Puente, F. Leteurtre, E. Gravel, N. Tassali, C. Boutin, E. Léonce, Y. Boulard, P. Berthault, B. Rousseau, *Chem. Eur. J.* **2013**, *19*, 6089–6093.
[44] E. Vedejs, P. L. Fuchs, *J. Am. Chem. Soc.* **1973**, *95*, 822–825.
[45] L.-L. Chapellet, J. R. Cochrane, E. Mari, C. Boutin, P. Berthault, T. Brotin, *J. Org. Chem.* **2015**, *80*, 6143–6151.
[46] M. Darzac, T. Brotin, L. Rousset-Arzel, D. Bouchu, J.-P. Dutasta, *New J. Chem.* **2004**, *28*, 502–512.
[47] O. Baydoun, T. Buffeteau, N. Daugey, M. Jean, N. Vanthuyne, L.-L. Chapellet, N. De Rycke, T. Brotin, *Chirality* **2019**, *31*, 481–491.
[48] O. Baydoun, N. De Rycke, E. Léonce, C. Boutin, P. Berthault, E. Jeanneau, T. Brotin, *J. Org. Chem.* **2019**, *84*, 9127–9137.
[49] T. Brotin, D. Cavagnat, E. Jeanneau, T. Buffeteau, *J. Org. Chem.* **2013**, *78*, 6143–6153.
[50] T. Brotin, N. Vanthuyne, D. Cavagnat, L. Ducasse, T. Buffeteau, *J. Org. Chem.* **2014**, *79*, 6028–6036.
[51] T. Brotin, E. Jeanneau, P. Berthault, E. Léonce, D. Pitrat, J.-C. Mulatier, *J. Org. Chem.* **2018**, *83*, 14465–14471.
[52] E. Léonce, J.-P. Dognon, D. Pitrat, J.-C. Mulatier, T. Brotin, P. Berthault, *Chem. Eur. J.* **2018**, *24*, 6534–6537.
[53] T. Brotin, P. Berthault, D. Pitrat, J.-C. Mulatier, *J. Org. Chem.* **2020**, *85*, 9622–9630.
[54] T. Brotin, P. Berthault, K. Chighine, E. Jeanneau, *ACS Omega* **2022**, *7*, 48361–48371.
[55] E. Léonce, T. Brotin, P. Berthault, *Phys. Chem. Chem. Phys.* **2022**, *24*, 24793–24799.
[56] T. Brotin, N. Daugey, J. Kapitan, N. Vanthuyne, M. Jean, E. Jeanneau, T. Buffeteau, *J. Org. Chem.* **2023**, *88*, 4829–4832.
[57] O. Della-Negra, Y. Cirillo, T. Brotin, J.-P. Dutasta, P.-L. Saaidi, B. Chatelet, A. Martinez, *Chem. Commun.* **2022**, *58*, 3330–3333.
[58] J. Canceill, L. Lacombe, A. Collet, *J. Am. Chem. Soc.* **1985**, *107*, 6993–6996.
[59] P. Satha, G. T. Illa, S. Hazra, C. S. Purohit, *ChemistrySelect* **2017**, *2*, 10699–10703.
[60] M. Doll, P. Berthault, E. Léonce, C. Boutin, T. Buffeteau, N. Daugey, N. Vanthuyne, M. Jean, T. Brotin, N. De Rycke, *J. Org. Chem.* **2021**, *86*, 7648–7658.
[61] C. Garcia, J. Malthete, A. Collet, *Bull. Soc. Chim. Fr.* **1993**, *130*, 93–95.
[62] C. Vigier, D. Fayolle, H. El Siblani, J. Sopkova de Oliveira Santos, F. Fabis, T. Cailly, E. Dubost, *Angew. Chem. Int. Ed.* **2022**, *61*, e202208580.
[63] C. Vigier, P. Fossé, F. Fabis, T. Cailly, E. Dubost, *Adv. Synth. Catal.* **2021**, *363*, 3756–3761.
[64] T. Traoré, L. Delacour, S. Garcia-Argote, P. Berthault, J.-C. Cintrat, B. Rousseau, *Org. Lett.* **2010**, *12*, 960–962.
[65] T. Traoré, L. Delacour, N. Kotera, G. Merer, D.-A. Buisson, C. Dupont, B. Rousseau, *Org. Process Res. Dev.* **2011**, *15*, 435–437.
[66] A. I. Joseph, G. El-Ayle, C. Boutin, E. Léonce, P. Berthault, K. T. Holman, *Chem. Commun.* **2014**, *50*, 15905–15908.
[67] a) C. J. Sumby, M. J. Hardie, *Angew. Chem. Int. Ed.* **2005**, *44*, 6395–6399; b) C. J. Sumby, J. Fisher, T. J. Prior, M. J. Hardie, *Chem. Eur. J.* **2006**, *12*, 2945–2959; c) M. J. Hardie, *Chem. Lett.* **2016**, *45*, 1336–1346.
[68] T. Wang, Y.-F. Zhang, Q.-Q. Hou, W.-R. Xu, X.-P. Cao, H.-F. Chow, D. Kuck, *J. Org. Chem.* **2013**, *78*, 1062–1069.
[69] D. Xu, R. Warmuth, *J. Am. Chem. Soc.* **2008**, *130*, 7520–7521.
[70] C. Givelet, J. Sun, D. Xu, T. J. Emge, A. Dhokte, R. Warmuth, *Chem. Commun.* **2011**, *47*, 4511–4513.
[71] M. A. Little, J. Donkin, J. Fisher, M. A. Halcrow, J. Loder, M. J. Hardie, *Angew. Chem. Int. Ed.* **2012**, *51*, 764–766.
[72] J. Sanseverino, J.-C. Chambron, E. Aubert, E. Espinosa, *J. Org. Chem.* **2011**, *76*, 1914–1917.
[73] M. A. Little, M. A. Halcrow, M. J. Hardie, *Chem. Commun.* **2013**, *49*, 1512–1514.
[74] F. Brégier, O. Hudeček, F. Chaux, M.-J. Penouilh, J.-C. Chambron, P. Lhoták, E. Aubert, E. Espinosa, *Eur. J. Org. Chem.* **2017**, *2017*, 3795–3811.
[75] Z. Zhong, A. Ikeda, S. Shinkai, S. Sakamoto, K. Yamaguchi, *Org. Lett.* **2001**, *3*, 1085–1087.
[76] J. J. Henkelis, T. K. Ronson, L. P. Harding, M. J. Hardie, *Chem. Commun.* **2011**, *47*, 6560–6562.
[77] a) T. K. Ronson, H. Nowell, A. Westcott, M. J. Hardie, *Chem. Commun.* **2011**, *47*, 176–178; b) V. E. Pritchard, D. Rota Martir, S. Oldknow, S. Kai, S. Hiraoka, N. J. Cookson, E. Zysman-Colman, M. J. Hardie, *Chem. Eur. J.* **2017**, *23*, 6290–6294; c) N. J. Cookson, J. M. Fowler, D. P. Martin, J. Fisher, J. J. Henkelis, T. K. Ronson, F. L. Thorp-Greenwood, C. E. Willans, M. J. Hardie, *Supramol. Chem.* **2018**, *30*, 255–266; d) E. Britton, R. J. Ansell, M. J. Howard, M. J. Hardie, *Inorg. Chem.* **2021**, *60*, 12912–12923; e) J. J. Henkelis, C. J. Carruthers, S. E. Chambers, R. Clowes, A. I. Cooper, J. Fisher, M. J. Hardie, *J. Am. Chem. Soc.* **2014**, *136*, 14393–14396.
[78] a) A. Schaly, Y. Rousselin, J.-C. Chambron, E. Aubert, E. Espinosa, *Eur. J. Inorg. Chem.* **2016**, *2016*, 832–843; b) A. Schaly, M. Meyer, Chambron, Jean-Claude, M. Jean, N. Vanthuyne, E. Aubert, E. Espinosa, N. Zorn, E. Leize-Wagner, *Eur. J. Inorg. Chem.* **2019**, *2019*, 2691–2706.
[79] A. Bouchet, T. Brotin, D. Cavagnat, T. Buffeteau, *Chem. Eur. J.* **2010**, *16*, 4507–4518.
[80] a) T. Brotin, D. Cavagnat, T. Buffeteau, *J. Phys. Chem. A* **2008**, *112*, 8464–8470; b) A. Bouchet, T. Brotin, M. Linares, H. Ågren, D. Cavagnat, T. Buffeteau, *J. Org. Chem.* **2011**, *76*, 1372–1383; c) T. Brotin, R. Montserret, A. Bouchet, D. Cavagnat, M. Linares, T. Buffeteau, *J. Org. Chem.* **2012**, *77*, 1198–1201.
[81] J. Jayapaul, L. Schröder, *Molecules* **2020**, *25*, 4627.
[82] R. M. Fairchild, A. I. Joseph, K. T. Holman, H. A. Fogarty, T. Brotin, J.-P. Dutasta, C. Boutin, G. Huber, P. Berthault, *J. Am. Chem. Soc.* **2010**, *132*, 15505–15507.
[83] T. Traoré, G. Clavé, L. Delacour, N. Kotera, P.-Y. Renard, A. Romieu, P. Berthault, C. Boutin, N. Tassali, B. Rousseau, *Chem. Commun.* **2011**, *47*, 9702–9704.
[84] E. Dubost, N. Kotera, S. Garcia-Argote, Y. Boulard, E. Léonce, C. Boutin, P. Berthault, C. Dugave, B. Rousseau, *Org. Lett.* **2013**, *15*, 2866–2868.
[85] a) G. K. Seward, Y. Bai, N. S. Khan, I. J. Dmochowski, *Chem. Sci.* **2011**, *2*, 1103–1110; b) K. K. Palaniappan, R. M. Ramirez, V. S. Bajaj, D. E. Wemmer, A. Pines, M. B. Francis, *Angew. Chem. Int. Ed.* **2013**, *52*, 4849–4853.
[86] N. Kotera, N. Tassali, E. Léonce, C. Boutin, P. Berthault, T. Brotin, J.-P. Dutasta, L. Delacour, T. Traoré, D.-A. Buisson, F. Taran, S. Coudert, B. Rousseau, *Angew. Chem. Int. Ed.* **2012**, *51*, 4100–4103.

[87] N. Kotera, E. Dubost, G. Milanole, E. Doris, E. Gravel, N. Arhel, T. Brotin, J. P. Dutasta, J. Cochrane, E. Mari, C. Boutin, E. Léonce, P. Berthault, B. Rousseau, *Chem. Commun.* **2015**, *51*, 11482–11484.
[88] E. Mari, Y. Bousmah, C. Boutin, E. Léonce, G. Milanole, T. Brotin, P. Berthault, M. Erard, *ChemBioChem* **2019**, *20*, 1450–1457.
[89] G. Milanole, B. Gao, A. Paoletti, G. Pieters, C. Dugave, E. Deutsch, S. Rivera, F. Law, J.-L. Perfettini, E. Mari, E. Léonce, C. Boutin, P. Berthault, H. Volland, F. Fenaille, T. Brotin, B. Rousseau, *Bioorg. Med. Chem.* **2017**, *25*, 6653–6660.
[90] J. Sloniec, M. Schnurr, C. Witte, U. Resch-Genger, L. Schröder, A. Hennig, *Chem. - Eur. J.* **2013**, *19*, 3110–3118.
[91] F. Rossella, H. M. Rose, C. Witte, J. Jayapaul, L. Schröder, *ChemPlusChem* **2014**, *79*, 1463–1471.
[92] S. Klippel, J. Döpfert, J. Jayapaul, M. Kunth, F. Rossella, M. Schnurr, C. Witte, C. Freund, L. Schröder, *Angew. Chem. Int. Ed.* **2014**, *53*, 493–496.
[93] R. Tyagi, C. Witte, R. Haag, L. Schröder, *Org. Lett.* **2014**, *16*, 4436–4439.
[94] J. Jayapaul, L. Schröder, *Bioconjug. Chem.* **2018**, *29*, 4004–4011.
[95] E. Siurdyban, T. Brotin, K. Heuzé, L. Vellutini, T. Buffeteau, *Langmuir* **2014**, *30*, 14859–14867.
[96] Q. Guo, Q. Zeng, W. Jiang, X. Zhang, Q. Luo, X. Zhang, L.-S. Bouchard, M. Liu, X. Zhou, *Chem. - Eur. J.* **2016**, *22*, 3967–3970.
[97] a) Z.-j. Chen, H.-w. Ai, *Biochem.* **2014**, *53*, 5966–5974; b) S. K. Bae, C. H. Heo, D. J. Choi, D. Sen, E.-H. Joe, B. R. Cho, H. M. Kim, *J. Am. Chem. Soc.* **2013**, *135*, 9915–9923.
[98] S. Yang, W. Jiang, L. Ren, Y. Yuan, B. Zhang, Q. Luo, Q. Guo, L.-S. Bouchard, M. Liu, X. Zhou, *Anal. Chem.* **2016**, *88*, 5835–5840.
[99] Q. Zeng, Q. Guo, Y. Yuan, Y. Yang, B. Zhang, L. Ren, X. Zhang, Q. Luo, M. Liu, L.-S. Bouchard, X. Zhou, *Anal. Chem.* **2017**, *89*, 2288–2295.
[100] Q. Zeng, Q. Guo, Y. Yuan, X. Zhang, W. Jiang, S. Xiao, B. Zhang, X. Lou, C. Ye, M. Liu, L.-S. Bouchard, X. Zhou, *ACS Appl. Bio Mater.* **2020**, *3*, 1779–1786.
[101] H. Zhang, Q. Yu, Y. Li, Z. Yang, X. Zhou, S. Chen, Z.-X. Jiang, *Chem. Commun.* **2020**, *56*, 3617–3620.
[102] B. A. Riggle, Y. Wang, I. J. Dmochowski, *J. Am. Chem. Soc.* **2015**, *137*, 5542–5548.
[103] O. Taratula, Y. Bai, E. L. D'Antonio, I. J. Dmochowski, *Supramol. Chem.* **2015**, *27*, 65–71.

Manuscript received: October 12, 2023
Revised manuscript received: December 27, 2023
Accepted manuscript online: December 28, 2023
Version of record online: January 22, 2024